Biosynthesis of Co_3O_4 and ZnO Nanoparticles Using *Ehretia cymosa thonn* Plant Leaf Extract: Comparative Study of Their Antibacterial Activity

Marta Hika Shoro

A Thesis Submitted to the Department of Applied Chemistry

School of Applied Natural Science

Presented in Partial Fulfillment of the Requirement for the Degree of Master's in

Applied Chemistry (Industrial Chemistry)

Office of Graduate Studies

Adama Science and Technology University

Jan, 2022

Adama, Ethiopia

Biosynthesis of Co_3O_4 and ZnO Nanoparticles Using *Ehretia cymosa thonn* Plant Leaf Extract: Comparative Study of Their Antibacterial Activity

Marta Hika Shoro

Advisor: Gemechu Deressa (PhD)

A Thesis Submitted to the Department of Applied Chemistry

School of Applied Natural Science

Presented in Partial Fulfillment of the Requirement for the Degree of Master's in Applied Chemistry (Industrial Chemistry)

Office of Graduate Studies

Adama Science and Technology University

Jan, 2022

Adama, Ethiopia

DECLARATION

I hereby declare that this Master Thesis entitled "**Biosynthesis of Co_3O_4 and ZnO Nanoparticles Using *Ehretia cymosa thonn* Plant Leaf Extract: Comparative Study of Their Antibacterial Activity**" is my original work. That is, it has not been submitted for the award of any academic degree, diploma or certificate in any other university. All sources of materials that are used for this thesis have been duly acknowledged through citation

Marta Hika Shoro — Name of student

Signature

07/02/2022 — Date

RECOMMENDATION OF ADVISORS

I, the advisor of this thesis, hereby certify that I have read the revised version of the thesis entitled "**Biosynthesis of Co_3O_4 and ZnO Nanoparticles Using *Ehretia cymosa thonn* Plant Leaf Extract: Comparative Study of Their Antibacterial Activity**" prepared under my guidance by **Marta Hika**. Therefore, I recommend the submission of the research to the department for further review and evaluation.

Gemechu Dereje (PhD) _____ 06/02/2022

Advisor Signature Date

APPROVAL SHEET

I, the advisor of the thesis entitled **"Biosynthesis of Co_3O_4 and ZnO Nanoparticles Using *Ehretia cymosa thonn Plant* Leaf Extract: Comparative Study of their Antibacterial Activity"** and developed by **Marta Hika**, hereby certify that the recommendation and suggestions made by the board of examiners are appropriately incorporated into the final version of the thesis.

Gemechu Degessa (PhD) _____ 06(02)2022

Advisor: Signature Date

We, the undersigned, members of the Board of Examiners of the thesis by **Marta Hika** have read and evaluated the thesis entitled **"Biosynthesis of Co_3O_4 and ZnO Nanoparticles Using *Ehretia cymosa thonn* Plant Leaf Extract: Comparative Study of their Antibacterial Activity"** and examined the candidate during open defense. This is, therefore, to certify that the thesis is accepted for partial fulfillment of the requirement of the degree of Master of Science in Applied Chemistry.

Aschalew Tadesse (PhD) _____ 09/02/2022

Chairperson Signature Date

Tegene Desalegn (phD) _____ 09/02/2022

Internal Examiner Signature Date

Mulatu K (phD) _____ 7 Feb 2022

External Examiner Signature Date

Final approval and acceptance of the thesis is contingent upon submission of its final copy to the Office of Postgraduate Studies (OPGS) through the Department Graduate Council (DGC) and School Graduate Committee (SGC).

Aschalew Tadesse Margiya(PhD) _____ 09/02/2022

Department Head Signature Date

Tegene Desalegn Zeleke (PhD) _____ 09/02/2022

School Dean Signature Date

Legesse Lemecha Obsu (Ph.D) _____ 09/02/22

Office of Postgraduate Studies, Dean Signature Date

Post Graduate Office Dean

TABLE OF CONTENT

CONTENTS Page

LIST OF TABLES

LIST OF FIGURES

LIST OF ABBREVIATION AND ACRONYMS

Co_3O_4 NPs	Cobalt Oxide Nanoparticles
DNA	Deoxyribonucleic Acid
eV	Electron Volt
FTIR	Fourier Transform Infrared Spectroscopy
nm	nanometer
ROS	Reactive Oxygen Species
SEM	Scanning Electron Microscopy.
UV-Vis	Ultra violet visible spectroscopy
WHO	World Health Organization
XRD	X-Ray Diffraction
ZnO NPs	Zinc Oxide Nanoparticles

ABSTRACT

Biosynthesis method using plant extract is a low cost and novel approach that is used to develop a variety of nanoparticles (NPs) that have numerous applications. In this work, cobalt oxide and zinc oxide nanoparticles were synthesized within 1:2, 1:1, and 2:1 volume ratios using their corresponding precursor salt and *Ehretia cymosa thonn* leaf extract that act as a reducing and capping agent to get stable NPs. Furthermore, the synthesized nanoparticles were characterized using X-Ray diffraction (XRD), scanning electron microscopy (SEM), Fourier transform infrared (FT-IR) spectroscopy and Ultra visible (UV-Vis) spectroscopic techniques, in order to get and gather as well confirm the formation of the NPs. The XRD analysis showed that ZnO NPs were highly crystalline, pure and the average crystalline size for the 1:2, 1:1, and 2:1 volume ratios were 22.96, 17.92, and 21.80 nm, respectively. In the same manner, the average crystal size and purity of the green formed Co_3O_4 NPs in the ratios of 1:2. 1:1, and 2:1 were found to be 22.14, 11.19, and 14.58 nm, respectively. SEM image analysis indicates surface morphology and all of the three ratios of ZnO NPs were found to be hexagonal in shape. Of the three ratios, ZnO (1:1) found to be more homogeneous. Likewise, the SEM analysis of Co_3O_4 NPs reveals the shape and morphology of the various volume ratios of Co_3O_4 NPs were found to be cubic. The UV-Vis analysis proves the optical property and so, the calculated band gap energy were found to be found 3.34, 3.27, and 3.25 eV for the 1:1, 2:1, and 1:2 volume ratios, respectively. While the band gap energy of Co_3O_4 NPs were found as 3.77, 3.70, and 3.55 eV for the $1:1, 1:2$, and $2:1$, respectively. The FTIR analysis shows the interaction between the extract with ZnO and Co_3O_4 NPs and the analysis proves as it contains several functional groups of bioactive molecules such as flavonoid, ketone, carboxylic acid, and alcohol, saturated and unsaturated hydrocarbons. The antibacterial activity for the (2:1, 1:1, and 1:2) was investigated using S. *Aureus* and *E. coli* within three concentrations of 50, 75, and 100 µg/mL. The antibacterial activities increase with increasing the concentration of ZnO NPs. In the same fashion, the antibacterial efficiency of synthesized Co_3O_4 NPs was tested for *S. Aureus* and *E. coli* using 50 µg/mL, 75 µg/mL, and 100 µg/mL concentration. Co_3O_4 $(2:1)$ shows zone of inhibition of 7, 13, 16 and 7, 12 and 15 mm for *E. coli* and *S. Aureus*, respectively. Co_3O_4 $(1:1)$ shows zone of inhibition of 8, 9, 10 and 9, 10 and 11 mm against *E. coli* and *S. Aureus*. Finally, Co_3O_4 $(1:2)$ with the same concentration showed zone of inhibition of 9, 11, 12 and 9, 11, 13 mm against *E. coli* and *S. Aureus*, respectively.

Keyword*:* Co_3O_4 and ZnO nanoparticles, *Ehretia cymosa thonn*, Biosynthesis, Antibacterial

1. INTRODUCTION

1.1. Background of the Study

Nowadays, bacterial resistance to antibacterial drugs is a critical health challenge worldwide that is associated with high morbidity and mortality. The major difficulty that faces antibacterial drug development is differentiating new drug-like compounds with its potent antibacterial activity. At the turn of the last century Salvarsan for the treatment of syphilis and the sulfonamides that target p-aminobenzoic acid biosynthesis was identified (Agarwal *et al*., 2018). In spite of the initial supremacy of synthetic antimicrobial drugs, there have been organic antibacterial drugs that have dominated as the preferred chemical scaffolds of antibacterial drugs since the middle of the last century. Several antibiotics were widely synthesized and used in treatment of bacterial caused infections (Happy *et al*., 2019).

Since the 1940s, antibacterial agents have greatly reduced illness and death from infectious diseases. However, along with using antibacterial drugs, bacteria become resistant against the antibiotics and make the drug less effective. Due to this, researchers explore various routes to solve the problems. With the development of nanotechnology, inorganic nanomaterials such as metal and metal oxide nanoparticles, have emerged as promising candidates due to their low toxicity, heat resistance and higher thermal stability when compared to organic compounds. Nanotechnology provides a good platform to develop metal oxides nanoparticles that have the potential for bacterial infectious diseases. Several metal oxides nanoparticles such as Fe_3O_4 (Ankamwar *et al*., 2010); (Durgadevi & Mani, 2018), MgO (Prasanth *et al*., 2019), TiO_2 (Aravind *et al*., 2021), ZnO (Saranya *et al*., 2017), Co_3O_4 and MnO_2 (Hafeez *et al*., 2020) were studied for the treatment of various human pathogen drug resistant. Of them, ZnO and Co_3O_4 nanoparticles attract researcher's interest due to their suitable physicochemical properties that enables for the efficient treatment of numerous bacteria caused infectious diseases. However, the antibacterial activity of *Ehretia cymosa thonn* leaf mediated synthesized ZnO and Co_3O_4 nanoparticles were not yet reported.

Nanotechnology deals with synthesis and various applications of nano size particles (1-100 nm) such as photocatalytic, energy conversion, sensor, adsorption, and finger print, cosmotic, electrical, agricultural, pharmaceutical and biomedical. These metal oxide nanoparticles could fabricated by physical, chemical and biological approaches (green synthesis). However, physical and chemical methods have certain disadvantages due to involvement of expensive and hazardous chemicals, high-energy requirements and radiation (Asamoah *et al*., 2020). Therefore, to solve these drawbacks, the green synthesis method is now utilized on a large scale. Green synthesis of nanoparticles is an approach of synthesizing nanoparticles using microorganisms, algae and plants having biomedical applications. This approach is biocompatible,

non-toxic, cost effective, highly stable, and fast, an environment friendly and does not required high temperature, heat toxic and hazardous chemicals due to these properties green synthesis methods are more approachable and superior than chemical and physical approaches ((Nasrollahzadeh *et al*., 2017).

Among the living organisms using for nanoparticles synthesis, plant can be advantageous over other biological processes because synthesis of nanoparticles by using microorganisms is somewhat difficult due to involvement of elaborate process of maintaining cell cultures, intra-cellular synthesis, required longer incubation time in the growth media for reducing a metal ion, water-soluble phytochemicals do the same in a moment, multiple purification steps and separation is not efficient. However, plant-mediated synthesis is suitable process for large-scale production of metal oxide nanoparticles rapidly and efficiently (Ren *et al*., 2009) and due to the presence of primary metabolites like polysaccharides, proteins, amino acids, organic acids and secondary metabolites (phytochemicals) like polyphenols, flavonoids, terpenoids, alkaloids, tannins, steroid and glycosides substances in plant extracts that can reduce size and stabilize the NPs (Annu *et al*., 2018); (Mittal *et al*., 2013); (Jamdagni *et al*., 2018),

Nowadays, several nanoparticles such as Co_3O_4, CuO, Fe_3O_4, TiO_2, WO_2 and ZnO nanoparticles were synthesized using plant extract. Among these, Co_3O_4 and ZnO nanoparticles attract researcher's interest due to their potent application in different fields. However, Co_3O_4 and ZnO nanoparticles were not synthesized using *Ehretia cymosa thonn* leaf extract. Cobalt oxide and zinc oxide nanoparticles exhibit attractive antibacterial properties due to increased specific surface area as the reduced particle size leads to enhanced particle surface reactivity (Siddiqi & Husen, 2016). Therefore, the aim of this study was to synthesis Co_3O_4 and ZnO nanoparticles using *Ehretia cymosa thonn* leaf extract and compare their antibacterial activity against Gram-ve (*Escherichia coli)* and Gram +ve (*Bacillus subtilis*).

1.2. Statement of the Problem

Recently, the antimicrobial activity of commercially available and chemically synthesized cobalt oxide and zinc oxide nanoparticles were studied. But, the methods used for synthesis of these nanoparticles are not environmentally friendly and cost effective. Due to this, researchers become interested in designing a new method called green synthesis which is non-toxic, low cost environmentally benign and rapid synthesis. There are several reports of green synthesized Cobalt oxide and zinc oxide nanoparticles with their numerous applications. However, *Ehretia cymosa thonn* plant leaf Extract mediated cobalt oxide and Zinc oxide NPs was not yet reported before this work. Under developed countries hospital-associated infectious diseases are a serious global challenge to human health particularly in children and old-age peoples. These bacterial-caused infectious diseases have been treated with several antibiotics. But, certain antibiotics have

been used widely and for a long period of time for bacterial infection treatments. Due to this, the bacteria become resistant to these antibiotics by developing genetic mutation or gene-trans mutation.

Thus, developing potent green method synthesized nanoparticles for antibacterial agents against bacteria strains mostly major pathogens including both gram negative and gram-positive strains has become an imperative issue worldwide. As reported before, different researches have done on the synthesis of cobalt oxide and Zinc oxide nanoparticles for antibacterial applications. However, the antibacterial activity of Co_3O_4 and ZnO NPs synthesized using *Ehretia cymosa thonn* plant leaf extract was not yet reported. For that reason, this work was focused on the green synthesis of cobalt oxide and zinc oxide nanoparticles using *Ehretia cymosa thonn* plant leaf extract and evaluate their potential antibacterial activity against gram negative and gram-positive strains.

1.3. Objectives

1.3.1. General objective

The general objective of this study was to synthesize Co_3O_4 and ZnO nanoparticles using *Ehretia cymosa thonn* leaf extract and compare their antibacterial Activity.

1.3.2. Specific objectives

- ✓ To synthesize Co_3O_4 and ZnO nanoparticles using *Ehretia cymosa thonn* plant Leaf extract.
- ✓ To characterize the synthesized nanoparticles using UV-visible, FT-IR, XRD and SEM techniques.
- ✓ To study the antibacterial activity of Co_3O_4 and ZnO nanoparticles against Gram-ve (*Escherichia coli*) and Gram +ve (*Bacillus subtilis*).
- ✓ To compare the antibacterial activity of Co_3O_4 and ZnO nanoparticles

1.4. Significance of the Study

This proposed study was provided valuable information on the green synthesis method of Co_3O_4 and ZnO nanoparticles using *Ehretia cymosa thonn* plant leaf extract, which is environmentally benign and antibacterial activity. This study was also provided scientific input regarding the antibacterial potential activities of *Ehretia cymosa thonn* plant leaf extract mediated cobalt oxide and zinc oxide nanoparticles. Additionally, this study was also provide perception for researchers on green synthesis of Co_3O_4 and ZnO nanoparticles using *Ehretia cymosa thonn* plant leaf extract for several applications.

1.5. Scope of the Study

This study was designed to synthesize cobalt oxide and zinc oxide nanoparticles by using *Ehretia cymosa thonn* plant leaf extract. The synthesized nanoparticles were characterized using instruments such as UV-Vis, SEM, FT-IR and XRD techniques. Finally, the antibacterial activities of *Ehretia cymosa thonn* plant leaf extract mediated synthesized Co_3O_4 and ZnO NPs were compared for both gram negative and positive bacteria strains.

2. LITERATURE REVIEW

2.1. Metal Oxide Nanoparticles

Metal oxide nanoparticles have recently gained enormous interest in various processes such as electron transistor devices, gas sensors, solar cells, pigments and waste water treatment etc., due to their unique optical, magnetic and electronic properties. Metal oxide nanoparticles such as cobalt oxide, copper oxide, silver oxide and zinc oxide nanoparticles are of great interest due to their excellent physical, chemical properties and their application in different fields, hence there is a notable research attention in the synthesis of various metal oxides nanoparticles. The conventional non-biological methods for their synthesis are not eco-friendly as they involve use of toxic reagents and also produce harmful by-products (Vasantharaj *et al*., 2019); (Asamoah *et al*., 2020). To overcome these limitations, green synthesis of metal nanoparticles was developed and gained research focus as these have significant biomedical applications. Nanoparticles are synthesized by both chemical and physical means for a long time, but the use of biological systems and microorganisms in the production of metal nanoparticles is under rapid growth in recent time owing to its greener route and ease of formation of nanoparticles. Recently there has been found much interest in the synthesis of nanoparticles by green means owing to their considerably improved properties over bulk metal (Vasantharaj *et al*., 2019); (Ahmad *et al*., 2019); (Rutberg *et al*., 2008)

2.1.1. Cobalt Oxide Nanoparticles

Cobalt has been known with allotropic forms including face centered cubic (FCC), Hexagonal centered phase (HCP), epsilon and body centered cubic (BCC). The FCC structure is thermodynamically preferred at higher temperatures and the HCP structure is favored at lower temperatures. The FCC structure appears to be stable phase even below room temperature when the particle sizes are smaller than 20 nm (Waris *et al*., 2021). There has been a considerable amount of research involving the preparation, structure and properties of magnetic cobalt nanoparticles in the past decade. The high magneto crystalline anisotropy of HCP Cobalt has spurred intensive studies of Cobalt based nanostructures for magnetic storage purposes. Cobalt nanoparticles coated with insulators have been prepared and studied for the applications in AC electrical and electronic devices (Zhang *et al*., 2019).

Different crystalline structures provide some practical benefits. Symmetrically structured FCC cobalt provides higher saturation moment and lower magnetic anisotropy which is suitable for linear applications such as converter. On the other hand, asymmetric HCP-cobalt has been a basic element for high temperature permanent magnets and suitable for microwave applications such as in circulator. Cobalt nanoparticles often possess mixed structures in which low energy stacking faults introduce a combination of FCC and HCP character making the synthesis of single structured cobalt a challenging task. The

potential applications of Cobalt oxide NPs in separation technology, catalysis, high-density magnetic recording and biomedicine are reviewed (Bibi *et al*., 2017).

The transition metal oxides have greatly attracted wide range of application in durable solar absorber lithium-ion battery. As transition metal groups cobalt oxide Co_3O_4 NPs is one of the most important materials because of its fascinating properties and thermal stability. Co_3O_4 NPs show good conductivity due to the existence of Co^{3+}. Co_3O_4 NPs synthesized by co-precipitation method is a simple process for the formation of nanoparticle and to control size of nanoparticles. Cobalt nanocrystals display a wealth of size-dependent structural magnetic, electronic and catalytic properties. The cobalt structure of p-type semiconducting materials with chemical stability at high temperature high mechanical strength and band gap 1.482.19 eV. Reported synthesis of Co_3O_4 nanoparticles at 750 ^{0}C using sol-gel method. Cobalt oxide nanoparticles were prepared in aqueous KOH solution with hydrothermal method have been studied electrical conductivity at different temperature (Raeisi *et al*., 2021).

2.1.2. Zinc Oxide Nanoparticles

Over the past few years, more interest is drawn towards zinc oxide NPs, since it has wider varieties of applications particularly in the fields of biomedical systems, optics, and electronics. Among all these types of metal oxides, ZnO NPs attract much attention because of their stimulating properties (such as the high direct bandwidth of 3.3 eV at room temperature and high excitation energies of 60 meV), optical property, high catalytic activity, anti-inflammatory, wound healing, and UV filtering properties. Several researchers have reported ZnO biosensors for cholesterol, enzyme biochemistry, and other biosensing applications (Choi & Choy, 2014); (Kolodziejczak-Radzimska & Jesionowski, 2014); (Demissie et al., 2020). Zinc oxide as a non-hygroscopic and nontoxic, inorganic, polar, crystalline material is a very cheap, safe, and readily available, which has aroused great interest in various organic transformations, sensors, transparent conductors, surface acoustic wave devices, production of microelectronic circuits, sensors, piezoelectric devices, fuel cells, surface passivation coatings, and corrosion catalysts (Uikey & Vishwakarma, 2016). Its activity depends on factors such as surface chemistry, size distribution, particle morphology, and particle reactivity in solution. It also used for drug delivery and as anticancer, ant-diabetics, antibacterial, antifungal and in cosmetics like sunscreen lotion due to its UV filtering properties (Kalpana & Devi Rajeswari, 2018). Several biosynthesized metal applications to biomedical and antimicrobial areas have been explored owing to their biocompatibility. Currently, researchers largely focus on the greener synthesis of ZnO nanoparticles with a particular focus on cancer therapy treatments.

2.2. Methods of Synthesis of Metal Oxide Nanoparticles

Numerous methods can be used for the synthesis of nanoparticles, but these methods are broadly categorized into two major classes, namely top-down and bottom-up approaches. The top-down approaches use macroscopic initial structures, which can be externally-controlled in the processing of nanostructures (Kalpana & Devi Rajeswari, 2018). Whereas, in bottom-up approach, green synthesis method utilizes the reducing and stabilizing agents present in the plant extracts which that results in formulation of stable and biocompatible nanoparticles. It uses molecular components that are built-up into assemblies (Waris *et al*., 2021); (Senthilkumar *et al*., 2017)

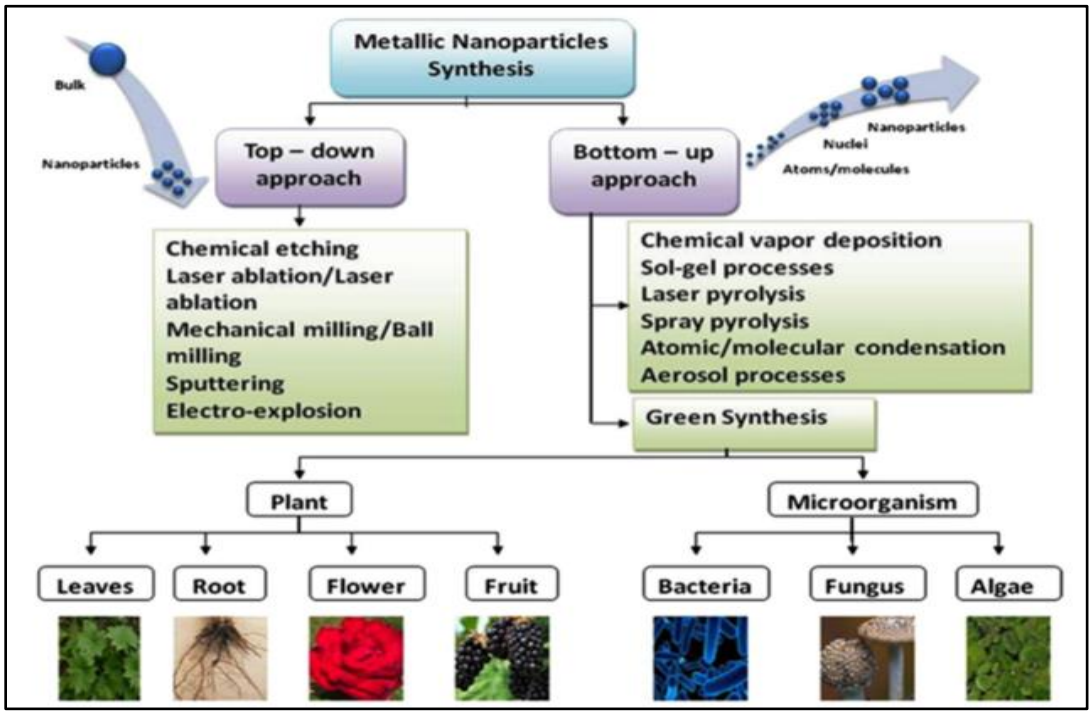

Figure 1. Methods of nanoparticles synthesis (Hussain *et al*., 2016)

The synthesis of metal oxide nanoparticles using green biological methods are favor for the synthesis comparing to physical and chemical methods that are very expensive, environment polluting, consuming more energy, sophisticated process, and time consuming process. Green methods are cost-effective, environmental friendly and easy process. Some basic principles of "green synthesis" can thus be explained by several components like prevention/minimization of waste, reduction of derivatives/pollution, and the use of safer (or non-toxic) solvent/auxiliaries as well as renewable feedstock. Among the available green methods of synthesis for metal oxide nanoparticles, utilization of plant extracts is a rather simple and easy process to produce nanoparticles at large scale relative to bacteria and/or fungi mediated synthesis. This is

due to the availability of effective phytochemicals in various plant extracts, especially in leaves (Ghosh *et al*., 2020).

In metal oxide nanoparticle synthesis using plant leaf extract, plant crude is mixed with metal precursor solutions at different reaction conditions in which plants crude for production of nanoparticle is beneficial over other biological processes. In this method, the solvent medium, environmentally benign reducing agent and the nontoxic material for the stabilization of the nanoparticles should have to be also evaluated.

As indicated in different studies the biomolecules also played in the capping of nanoparticles. Plant mediated synthesis of nanoparticles is conferred due to the presence of biomolecules such as proteins, amino acids, vitamins, polysaccharides, polyphenols, terpenoids, and organic acids such as citrates etc. (Happy *et al*., 2019); (Kalpana & Devi Rajeswari, 2018).

2.2.1. Green Synthesis of Co_3O_4 Nanoparticles

Extract from bio-organism may act both as reducing and capping agent in nanoparticles synthesis. The reduction of metals ions by bimolecular found in these extracts such as protein, polysaccharide, vitamin and amino acid is environmentally saved. Biological methods are regarded as safe, cost effective, sustainable and environmentally friendly processes for the synthesis of nanoparticles. Biological synthesis of nanoparticles is gaining importance due to its eco friendliness and simplicity. The use of plant materials in the synthesis of cobalt oxide nanoparticles has been reported by other researchers. These plant materials include the leaves of *Conocarpus erectus,* leaves of *Raphanussativus var. longipinnatus* and dried powdered fruits of piper longum (Hafeez *et al*., 2020).

Judhit Vijaya *at al*., synthesized 15 nm Co_3O_4 NPs using *Azadirechta indica* leaves extract and reported for the antimicrobial activity against gram positive and gram-negative bacteria (Pagar *et al*., 2019). Also, they applied Co_3O_4 NPs as a catalyst for the hydrogenation 4-nitrophenol and 4- nitroaniline. Sharma and co-workers reported biosynthesis of Co_3O_4 NPs using latex of *Calotropis procera* were in the size of 3-5 nm and analyzed the antibacterial activity of the prepared nanoparticles. Yulizar and co-workers synthesized Co_3O_4 NPs using *Euphorbia heterophylla* leaf extract and studied the photocatalytic activity of synthesized NPs. The synthesized NPs are spherical shape with the size ranges from 69.75 nm. They evaluated the photocatalytic activity of green synthesized Co_3O_4 NPs using methylene blue dye and results indicate Co_3O_4 NPs exhibits good photo catalytic activity (degraded up to 63.10%) under visible light irradiation (Dewi *et al*., 2019). Liu and co-workers described biosynthesis of Co_3O_4 NPs using leaf extract of *Gingko* were in the size of 30-100 nm. They successfully utilized Co_3O_4 NPs as direct electrochemical sensing interface for non-enzymatic detection of H_2O_2 and glucose. Saeed and co-workers synthesized plate shape

Co_3O_4 NPs using *Helianthus annus* leaf extract and studied the photocatalytic activity of synthesized Co_3O_4 NPs using methyl orange dye (Jia *et al*., 2016)

2.2.2. Green Synthesis of ZnO Nanoparticles

The synthesis of biological nanoparticles represents an alternative for the physical and chemical methods of nanoparticle formation. The majority of researchers focused on the green synthesis of nanoparticles for the formation of metal and oxide nanoparticles. The use of plants for the synthesis of nanoparticles is a rapid, low-cost, eco-friendly option and is safe for human use. *Vitex negundo* plant extract was used to produce ZnO NPs with zinc nitrate hexahydrate as a precursor. The biosynthesized ZnO NPs showed antimicrobial activities against *E. coli* and *S. aureus* bacteria. Dobrucka and Dugaszewska used *Trifolium pratense* to synthesize ZnO NPs (Dobrucka & Długaszewska, 2016). The synthesized ZnO NPs were found to be of hexagonal shape and the sizes were found to be of 60-70 nm. Kalpana *et al*. synthesized ZnO NPs using *Lagenaria siceraria* pulp extract. In addition, the researchers evaluated the biosynthesized ZnO nanoparticles for antidandruff, antimicrobial, and antiarthritic efficacy (Kalpana & Devi Rajeswari, 2018). Dhanemozhi *et al*. successfully synthesized the ZnO NPs from green tea leaf extract to evaluate their capacitance behavior for supercapacitor applications (Singh *et al*., 2018). ZnO NPs are known to be multifunctional inorganic nanoparticles with their major application in the treatment of urinary tract infection. Santhoshkumar *et al.* synthesized the ZnO NPs using *Passiflora caerulea* leaf extract and tested against the pathogenic culture isolated from the urine of the patient suffering from urinary tract infection (Santhoshkumar & Balupillai, n.d.). The results showed that the synthesized ZnO NPs act as an antibacterial agent against urinary tract infection. Nava *et al*. dealt with low-cost, nontoxic green synthesis of ZnO NPs prepared using *Camellia sinensis* extract (Navarro-Yepes *et al*., 2014). The efficiency of ZnO NPs as a photocatalyst for the degradation of various organic dyes such as methylene blue and methyl orange and their antioxidant activity by the DPPH assay has been studied by Siripireddy and Mandal using *Eucalyptus globulus*. The synthesis of monophase crystalline ZnO nanoparticles with a size range of about 15.8 nm by the green novel and environmentally friendly pathway using the extract of *A. betulina* as an effective oxidizing/reducing agent has been demonstrated for the first time by Thema *et al*. Stable and spherical ZnO NPs were produced by using zinc nitrate and *Aloe vera* leaf extract (Jiang *et al*., 2018).

2.3. Applications of Co_3O_4 and ZnO NPs

The Co_3O_4 and ZnO nanoparticles have become an important field of research over the past several decades with applications in various sectors, such as biomedical, pharmaceutical, industry, engineering, electronics, cosmetic, food and many others, because of their unique characteristics. Presently, these metal oxide

nanoparticles are one of the important nanoparticles with novel applications in variety of fields and they could be distinctive for the future technology of the coming decades. Moreover, they are used in medicine, for treatment of disease such diabetes, cancer, and microorganism borne diseases in health care. Therefore, the development of potent Co_3O_4 and ZnO nanoparticles with high surface area to volume ratio is the focus of the intense research, driven by strategies based on nanoscience and nanotechnology (Siddiqi *et al*., 2018, Rasmussen *et al*., 2010)

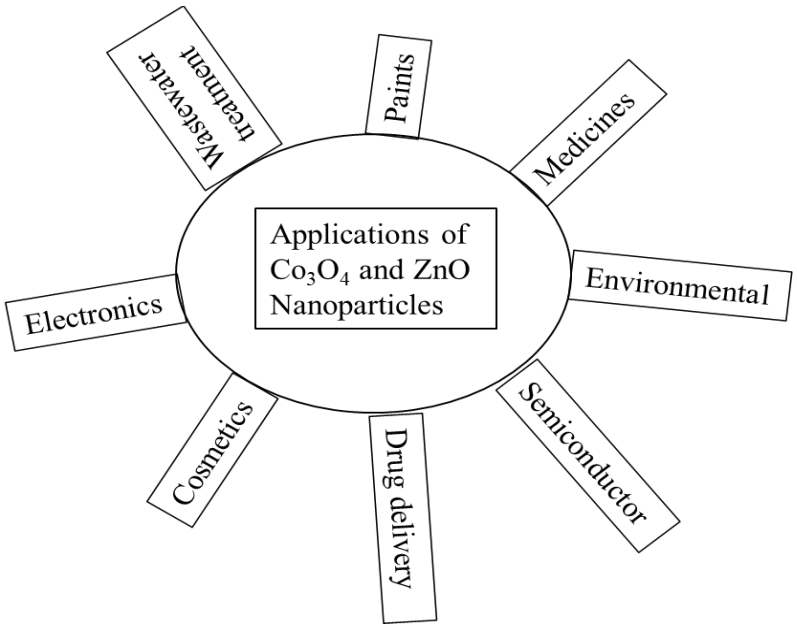

Figure 2. Different applications of Co_3O_4 and ZnO nanoparticles (Waris *et al*., 2021)

In addition to this, zinc oxide nanoparticles have been valued in various applications, such as sunscreens, toothpastes, and cosmetics especially because of their ability to absorb ultraviolet radiation (Huang *et al*., 2021, (Pavan Kumar *et al*., 2015).

2.4. Antibacterial Activity of Co_3O_4 and ZnO NPs

2.4.1. Antibacterial Activity of Co_3O_4 NPs

Metal based nanoparticles represent an alternative for biomedical treatments mainly in the fabrication of biomedical devices with antimicrobial coatings. A high antimicrobial activity of nanoparticles depends on the particle size that allows greater surface contact and a direct interaction with the membranes microorganisms. Nanoparticles smaller than 10 nm highly interact with bacteria and produce electronic effects which improve the reactivity of nanoparticles. Thus, it is proven that the bactericidal effects of nanoparticles is size dependent. The cell membranes of the microorganisms interact with the medium so metal oxide NPs have some interactions to release metal ions that interfere with the processes of the deoxyribonucleic acid (DNA)

replication, cell membrane formation and cell division. Several studies propose that nanoparticles attach to the surface of cell membrane disturbing the permeability and respiration function of the cell. The damage to the cell may be caused by the interaction of nanoparticles with sulfur or phosphorus containing bio molecules in the cell such as DNA (Matinise et al., 2018).

Therefore, sulfur containing proteins in the membrane or inside cells and phosphorus containing Molecule like DNA are likely to be preferential sites for binding NPs. The smaller nanoparticles have more antibacterial activity that provides more surface exposure to the bacterial membrane. In addition, these nano sized particles penetrate through cell membrane easier interacting with intracellular materials and finally resulting in cell destruction in the process of multiplication. Reports show that the nanoparticles induce oxidative stress to bacteria and induce reactive oxygen species (ROS) thus antibacterial activity could be explained based on ROS such as hydrogen peroxide (H_2O_2) Hydroxyl radicals (OH^-) and singlet oxygen (O^-). It is believed that microorganisms carry a negative charge while metal oxides carry a positive charge. This creates an electromagnetic attraction between the microbe and treated surface (Kiani *et al*., 2021); (Pagar *et al*., 2019).

Currently several antimicrobial drugs are used to kill microbe or prevent the growth of microbe However with the worldwide use and abuse of the most commonly used antibacterial drugs microorganisms especially bacteria are becoming resistant to more and more antimicrobial agents. For example bacteria strains known to be cause tuberculosis (TB) are found to be resistant to previous effective antibacterial treatment. *E. coli* is found to be intrinsically resistant to therapeutic level of penicillin G. The first beta lactam introduced into clinical practice because of its outer membrane barrier *E. coli* is also resistant to several different classes of antibiotics with distinct mechanism of action (Chen *et al*., 2010).

There are many advantages to using metal NPs as antimicrobial agents due to their stability, Robustness and self-life. Synthesis of cobalt oxide NPs for antibacterial activities has been reported by researchers from the leaves of *Conocarpuserectus,* leaves of *Raphanussativus var. longipinnatus* and dried powdered fruits of piper longum. Herein is reported the biofabrication of cobalt oxide nanoparticles using leaf of *Chromolaenaodorata* and their antibacterial application Nano sized cobalt oxide NPs have shown to possess antibacterial activities and several studies reported that they can be used as bactericides for water disinfection. The antibacterial activities of Cobalt oxide NPs against *E. coli* and *staphylococcus aureus* were examined. The performance of Cobalt oxide NPs for antibacterial activities prepared by biological and chemical methods towards microbes have not been studied well. Therefore, it is important to study comparison of biologically and chemically synthesized cobalt oxide NPs for antibacterial applications (Ajarem *et al*., 2021).

Hafeez et al., reported that the *Populus ciliate* plant leaf mediated Co_3O_4 NPs have good antibacterial activities against both gram positive and gram negative bacteria. The report showed antibacterial activities of Co_3O_4-NPs were higher against gram positive bacteria as compared to gram negative bacteria. Co_3O_4 NPs showed maximum inhibition zone 24.5 ± 1.3 and 20.4 ± 0.7) against gram positive bacteria (*B.subtillus*) and gram negative bacteria (*Klebsiella pneumoniae*) respectively. The reported data indicated that the activity of cobalt oxide NPs against *B.subtillus* was even higher than Bacitracin (the antibiotic used as a control. This ensured the potential activity of Co_3O_4 NPs against human pathogens (Hafeez et al., 2020).

2.4.2. Antibacterial Activity of ZnO NPs

In nanoscience, ZnO nanoparticles show a significant growth inhibition under normal laboratory lighting conditions and in the same time they have selective toxicity and are regarded as a safe reagent to humans and animals, this action can be understood because ZnO inhibiting the adhesion and internalization of bacteria and so ZnO can protect against intestinal diseases caused by *E. coli*. The morphological changes of *E. coli* treated with zinc oxide, which showed that ZnO nanoparticles could damage the membrane of these bacteria and so led to the leakage of cytosolic components and finally killed the bacterial cell. Zinc oxide nanoparticles have stronger antibacterial activity due to largely increased surface or enhanced the affinity. ZnO appeared that it has a significant antibacterial activity against a wide range of bacterial species and in particular against S. aureus. The antimicrobial property of ZnO nanoparticles also were analyzed with *K. pneumonia* and *B. subtilis* using agar well diffusion. It has been suggested that the mechanism of the antibacterial activity of ZnO NPs is based on its ability to induce oxidative stress. The Zn^+ ions released interact with the thiol group of the bacterial respiratory enzymes, increasing the production of reactive oxygen species (ROS) and causing oxidative stress in the bacterial cell. This oxidative stress damages the bacterial membranes, DNA, and mitochondria, resulting in the death of the bacteria. In addition, another feature that made ZnO nanoparticles compete other metal oxide nanoparticles is its antibacterial activity against a broad range of bacteria: gram positive and gram negative(Choi & Choy, 2014); (Wang *et al*., 2014); (Slman *et al*., 2018); (Abebe et al., 2020).

2.5. Drug Resistance Bacteria

Antibacterial resistance is the ability of a bacteria to resist the effects of drug that once could successfully treat the bacteria. Bacterial resistance occurs as a result of either natural or acquired mechanism. Natural resistance results when the properties of bacteria inhibit the action of a certain antibacterial. As reported earlier, an antibacterial designed to attach to certain specific receptors on a bacterial cell is unable to act if

the bacterial species does not have the receptors, while acquired resistance results due to change of bacterial species and its genetic makeup in such a manner that it decreases the action of antibacterial (Rice *et al*., 2019).

The release of metal ions from their corresponding metal oxide NPs is one of the main propositions in antibacterial mechanisms which are known to inhibit several bacterial cells activities including active transport, bacteria metabolism and enzymes activity. Subsequently, the toxicity properties of metal ions on the bacterial cell biomolecules induced the cell to death. Moreover, the release of metal ions is size and morphology dependent. Hood M. report that the Gram positive bacteria have a thick layer of peptidoglycan and have teichoic acid and lipoteichoic acid. This teichoic acid and lipoteichoic acid serve as chelating agent and also provide rigidity to the cell. They chelate Zn^{+2} ion from ZnO NPS complex and transport inside the cell. Whereas, the Gram negative bacteria have a triple layer of peptidoglycan in their cell wall where porins are present in the outer layer(Kalpana & Devi Rajeswari, 2018).

While the other proposed antibacterial activity is caused by the formation of reactive oxygen species (ROS) which leads to oxidative stress and subsequent cell damage or death which are generated under UV exposure an. Eventually, the H_2O_2 penetrates the bacterial membrane and damage the cellular components such as lipid, protein and DNA resulting in injuries and cells death (Pavan Kumar *et al*., 2015).

2.6. Chemistry of Ehretia cymosa thonn

Ehretia cymosa thonn is a deciduous shrub tree which growing up to 7 m tall in the western parts of its range, but can sometimes reach heights of 20-25 m recorded from different part of Africa. It is a glabrous shrub with ovate leaves and white flowers. The tree has a number of uses, supplying medicines, food and wood for the local population. It has potential for use as an ornamental. The fresh leaves are sometimes used in sauces. *Ehretia cymosa thonn* are used in traditional folklore medicine for treatment of diarrhea. The leaves have been used for treatment of measles (viral diseases) and also used as febrifuge, laxative and pain-killer as well as amelioration of paralysis, epilepsy, convulsions and spasm.

The medicinal role of *E. cymosa thonn* plant leaf is due to the presence of bioactive molecules such as alkaloids, saponins, glycosides, fatty acids, essential oils, reducing sugars, terpenoids, pseudotannins, anthraquinones, phenolics, steroids and flavonoids. In addition to this, the phytochemical constituents of *E. cymosa thonn* plant leaf have a potential activity in the treatment of diseases such antibacterial, antidiabetic, anti-inflammatory, anticancer, antifungal, antihyperglycaemic and antioxidant activities (Benhammada & Trache, 2021).

The antibacterial activity of ethanol solvent extract of *E. cymosa thonn* against *Bacillus subtilis* and *E. coli* using agar diffusion assay have reported (Sarkodie *et al*., 2015). Bagaje *et al*. (2017) also reported the

antibacterial activity of methanol solvent extracted *E. cymosa thonn* plant leaf against *Pseudomonas aeruginosa, Escherichia coli, Staphylococcus aureus* and *Proteus mirabilis* using well diffusion method with gentamicin and vancomycin as positive controls. The methanol extract of this plant leaf inhibit the *Escherichia coli and Staphylococcus aureus* with zone of 12.0 mm and 9 mm, respectively. The antidiabetic activity of different solvent extracted bioactive molecules of *E. cymosa thonn* plant leaf using α- amylase and α-glucosidase inhibitory assays have been reported (Ogundajo *et al*., 2016).

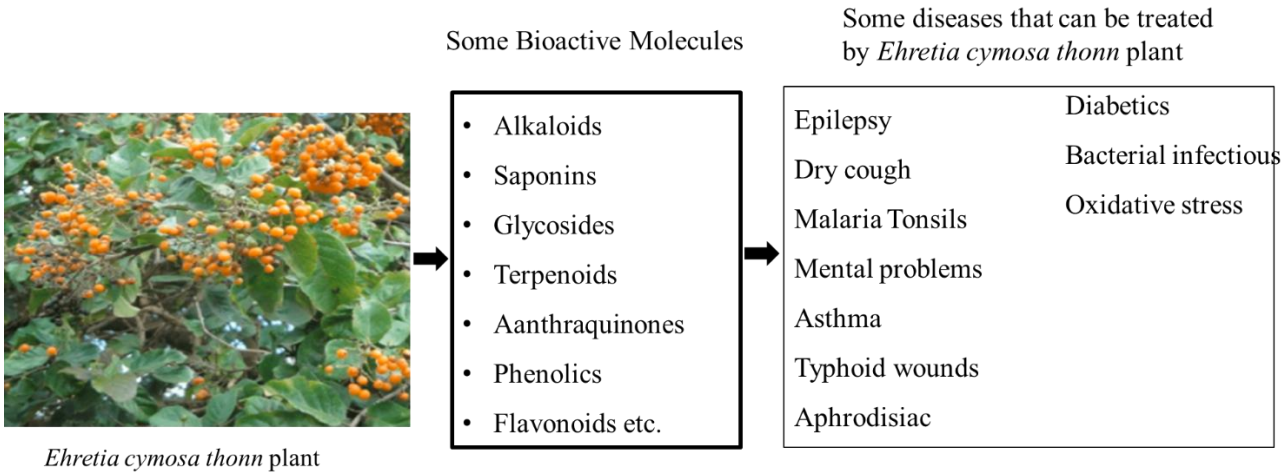

Figure 3. *Ehretia cymosa thonn* plant.

3. MATERIALS AND METHODS

3.1. Apparatus and Instruments

The apparatus and instruments used in this research work include: Oven, pH meter, magnetic stirrer, centrifuge, glass filters, plant grinding machine and hot plate. The instruments used include ultraviolate spectroscopy (UV-Vis), Scanning electron microscope (SEM) and X-ray diffraction spectroscopy (XRD) and Fourier transformer infrared (FTIR) spectroscopy.

3.2. Chemicals and Reagents

The chemicals, solvents, and reagents that were used in this study includes: cobalt nitrate hexahydrate $Co(NO_3)_2.6H_2O$) (Aldrich), zinc acetate dehydrate ($Zn(CH_3CO_2)_2{\cdot}2H_2O$) (Aldrich), double distilled water, Ethanol (97%), nutrient agar, Muller Hinton agar, HCl and NaOH. Those chemicals and reagents were used without any further purification.

3.3. Collection and Extraction of *Ehretia cymosa thonn* plant Leaf

The leaf of *Ehretia cymosa thonn* plant was collected from Adama city and washed carefully using distilled water to remove the dust particles. Then, the washed plant leaf was dried under shaded at room temperature to remove residual moisture content and make it ready for grinding. Then the leaf powder was packed within a plastic bottle followed by covering the whole body of the plastic bottle with aluminum foil. Extraction of the leaf was done by taking 40 g of leaf powder followed by adding 600 mL of distilled water and placing the mixed components on a hot plate. The mixed components were boiled at 60℃ for 90 min until the required suspension is formed. Then after, the extracted suspension was allowed room temperature cooling followed by filtering it and placing the filtrates within a refrigerator at 4℃. The filtrate extract was used as reducing and capping agent for the green synthesis of Co_3O_4 and ZnO nanoparticles (Wu *et al*., 2019).

3.4. Synthesis of Co_3O_4 and ZnO Nanoparticles

3.4.1. Synthesis of Co_3O_4 Nanoparticles

Cobalt nitrate hexahydrate (Co $(NO_3)_2.6H_2O$)) and leaf extract of *Ehretia cymosa thonn* plant was used for the synthesis of Co_3O_4 nanoparticles. To obtain ultra-fine nanoparticles of Co_3O_4, optimizations were performed and the well reduced Co_3O_4 nanosize was taken for further characterizations and applications. In synthesis, 0.5 M of $Co(NO_3)_2.6H_2O$) was prepared and mixed together within a reaction Erlenmeyer flask with plant leaf extract in 1:1, 1:2 and 2:1 volume ratio. A small sized magnetic bar was placed into the Erlenmeyer flask containing the extract and the precursor solution to enhance the reaction kinetics. The two components were then allowed to stir for about 4 hrs at room temperature without applying any heat

energy. After stirring time is completed, the pH of the formed suspensions were checked and controlled by adding some quantities of NaOH solution to 9.50. The resulting suspension was then stirred again for 20 min to maintain the uniform distribution of the added base. This basic solution was used to enhance precipitate formation and also to control pH of the suspension within the required range. The formed suspension was placed within a refrigerator overnight to enhance precipitation formation and then after the supernatant was decanted carefully followed by centrifugation at 12,000 rpm for 20 min followed by washing a minimum of three times using ethanol and distilled water. Then after, it was collected using a ceramic crucible dish followed by placing it into a drying oven for 3 hrs at 100 ℃ and then allowed to cool. Finally, each of the various ratios was calcined using a muffle furnace at 500 ℃ for 5 hrs. At the end, the nanoparticles were grinded and ready for further characterizations and analysis (Urabe & Aziz, 2019).

3.4.2. Synthesis of ZnO Nanoparticles

Zinc oxide nanoparticles was synthesized using 0.5 M of zinc acetate solution and leaf extract of *Ehretia cymosa thonn* plant in 1:1, 1:2 and 2:1 volume ratio for each concentration. The precursor salt solution and plant leaf extract were mixed within an Erlenmeyer flask. Then the mixed suspension containing a bar was allowed to be stirred for about 4 hrs by placing it on a magnetic stirrer without applying of heat. After completion of stirring time, pH of the suspension was checked using a pH meter and then after, a small amount of 1 M NaOH solution was added until the pH adjusted to 11.00 as a precipitating agent to enhance the formation of a precipitate and to control and manage pH of the formed suspension. Then after, the formed suspension was placed within a refrigerator for overnight in order to get excess precipitate. The resulted suspension was centrifuged at 4000 rpm for 20 min for about three times followed by washing with DH_2O and ethanol at each separated step. After that, the sample was allowed oven drying. Each volume ratios of the dried sample was calcined at 450 ℃ for 2 hrs using muffle furnace. At the end, the formed samples were grinded into powder and make it ready for characterization (Samy *et al*., 2019).

3.5. Characterization Methods

Characterization methods used include UV-Vis (JASCO, UV-Vis) (for the purpose of absorption analysis), scanning electron microscopy (JCM-6000Plus), Fourier transform infrared spectroscopy (PerkinElmer 65) and X-ray diffraction (XRD (XRD-7000, Shimadzu Co., South Korea).

3.6. Method of Antibacterial

3.6.1. Preparation of Inoculums for Antibacterial test

25 mg of nutrient agar was dissolved in 100 mL of distilled water in two labeled conical flasks and then was sterilized. In each conical flask clinically isolated strain of Gram-negative and positive bacteria was

inoculated and ready for the next activity. These bacterial cultures inoculated in nutrient broth, was allowed to be kept on rotary shaker for about 24 hrs at 100 rpm.

3.6.2. Disc diffusion method

The antibacterial activity of Co_3O_4 and ZnO nanoparticles were tested by using a disc diffusion method. The tests were performed using the suspension of bacteria spread on nutrient agar. Then the swab was dipped into the broth culture of the prepared bacteria strains and gently squeezed against the tube to remove excess fluid. The swab was used to streak the agar plate or a nutrient agar plate for a lawn of growth. The swab was used to streak the outside diameter of the agar; the inoculated plates were incubated at 37 ^{o}C for about 24 hrs. Then afterward, the antibiotic discs were placed on the surface of the agar using a dispenser that dispenses multiple discs at the correct distance apart or by obtaining individual discs and placing them on the surface of the agar using flame sterilized forceps. Then the antimicrobial activity was evaluated by measuring the diameter of the zone of inhibition against Gram-negative and positive strains using a ruler and calipers (Hafeez *et al*., 2020, A. Hussain *et al*., 2019).

4. RESULTS AND DISCUSSION

The crystallinity of ZnO and Co_2O_3 nano powders, morphological features, optical properties and behavior of functional group of both NPs were characterized by X-ray Diffractometer (XRD), Scanning Electron microscopic (SEM), Ultra visible (UV-Vis) spectroscopic techniques and Fourier Transform Infrared Spectroscopy (FT-IR), respectively.

4.1. XRD Analysis of ZnO and Co_3O_4 NPs

The X-ray diffraction (XRD) pattern of green synthesized ZnO NPs obtained from zinc acetate precursor and leaf extract of *Ehretia cymosa thonn* within three various volume ratios are illustrated in Figure 3. The diffraction peaks for the three ratios were found to be appeared at a 2θ value of ≈ 31.81°, 34.46°, 36.23°, 47.59°, 56.64°, 62.23°, 66.42°, 67.99°, and 69.01° for 7:3 ratios. 31.77, 34.41, 36.25, 47.54, 56.60, 56.60, 66.49, 67.97, and 69.08 for 4:1 ratio. 31.78, 34.45, 36.27, 47.57, 56.61, 62.46, 66.40, 67.96, 69.06 for 9:1 ratio. Corresponding to (100), (002), (101), (102), (110), (103), (200), (112), and (201) crystal planes, respectively. It has been found that, all the diffraction peaks approximately close to the reported information with the JCPDS file card No. of 00-76-0206, and the characteristic peaks for pure ZnO were observed in the XRD patterns confirming the formation of highly crystalline and dispersed ZnO NPs. The average crystalline of the green mediated synthesized ZnO NPs were found to be 20.95, 22.87, and 22.96 nm for the 7:3, 4:1, and 9:1 volume ratios of zinc precursor and leaf extract of *Ehretia cymosa thonn*, respectively. As can be confirmed from the spectra, no extra diffraction peaks of other phases are detected in the three volume ratios, indicating the phase purity of the green synthesized ZnO-NPs.

In the present study the average crystalline size of the green synthesized ZnO NPs found to be best as compared to the previously reported works. This further indicates the role of the leaf extract that controls the over growth of the synthesized ZnO NPs as a capping and stabilizing agent. The presence of the leaf extract as both a capping and reducing agent enhances and allows achieving small average crystalline size. Furthermore, the analysis confirms that the green-synthesized ZnO nanoparticles are in hexagonal with space group p63mc(186) structure without any impurities within the detection limits of XRD instrument and within the scanned region 10-80°. As the width of the peak increases, the size of the particle decreases, which resembles that the present studies of ZnO material is within the nano size range. In addition, the appearance of sharp diffraction patterns confirms the small size as well as high crystallinity of the synthesized nanoparticles. The average crystalline size of each of the three volume ratios of green synthesized ZnO NPs were found to be fit with its XRD spectra as indicated in Figure 3. It has been found

that as the extract of *Ehretia cymosa thonn* decreased, the average crystalline size was increased. However the 1:1 ratio average size was intermediate between the 7:3 ratio and 9:1 ratio. This is due to the fact that as less extract is added to the zinc precursor salt, it reduces less and so, the crystalline size of the obtained ZnO NPs was increased. Among the three ratios of ZnO, ZnO (1:1) NPs showed smaller average crystalline size as 17.92 nm compared to the remaining two ratios, this might be due to the presence of optimized amount of the extract; within the level of the coating surface of ZnO NPs. The remaining two ratios of ZnO NPs showed relatively large size and this might be contributed from the presence of small volume of extract (capping and reducing agent) it has been found that the 2:1 ratio contains 30% of the extract and its size is greater than the 1:1 ratio, implies that the over excess addition of extract might increase the size because it is beyond the coating surface of ZnO NPs, the study confirms that the best optimized ratio were to be 1:1 ratio.

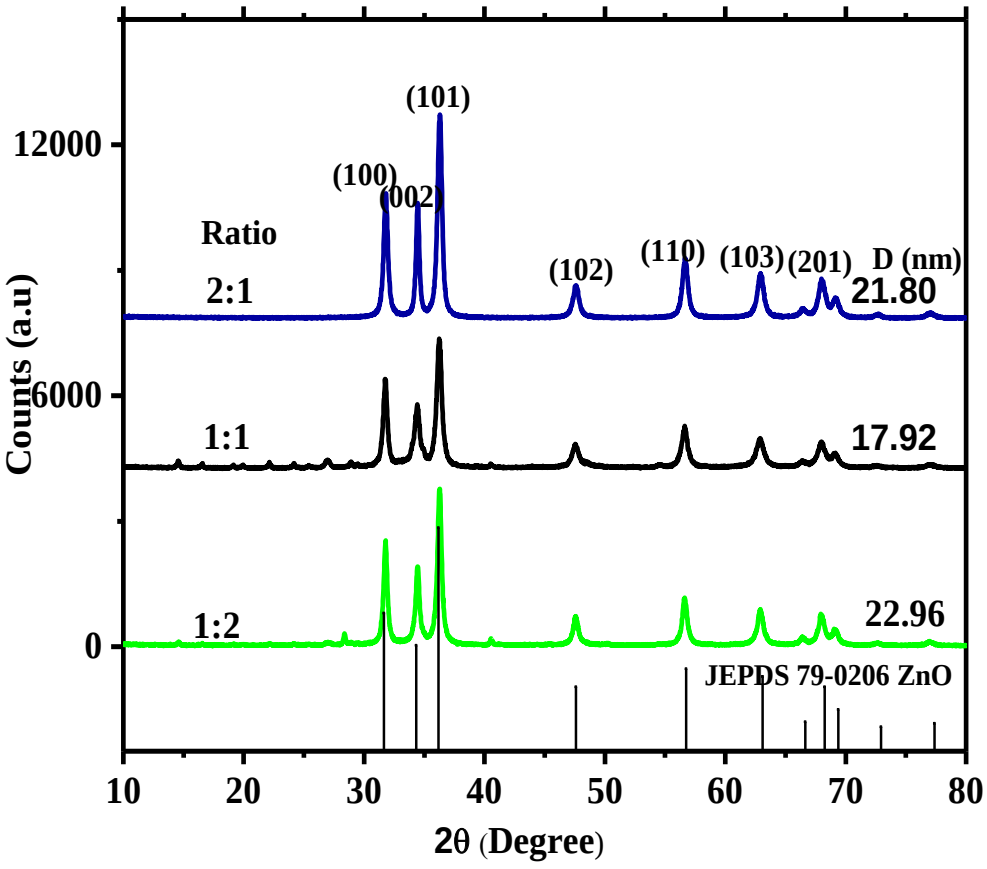

Figure 4. XRD spectra of *Ehretia cymosa thonn* mediated synthesized ZnO NPs.

Similarly, the formation of green synthesized Co_3O_4 NPs analysis of the crystal phases and average crystalline size of the synthesized Co_3O_4 nanoparticles prepared through green method using *Ehretia cymosa thonn* leaf extract within the 1:2, 1:1, and 2:1 volume ratios were done using X-ray diffractometer.

XRD data was taken for the prepared samples of Co_3O_4 NPs with X-ray diffractometer (XRD-7000, Shimadzu Co, Japan) at room temperature. Co_3O_4 NPs were formed from the reduction of cobalt (II) nitrate hexahydrate in the presence of *Ehretia cymosa thonn* leaf extract, which was act as a reducing, stabilizing and capping agent during the synthesis process. Figure 4 displays the XRD spectrum of *Ehretia cymosa thonn* leaf was extract mediated synthesized cobalt oxide NPs. The diffraction peaks of the green obtained Co_3O_4 (2:1) NPs were found to be located at ≈ 2θ of 19.58 31.39, 36.36, 38.67, 44.93, 55.77, 59.47, 65.34, 77.43 and 78.43 corresponded to the miller indices (hkl) value of 111, 220, 311, 222, 400, 422, 511, 440, 533 and 622, respectively. In the same manner the diffraction peaks of Co_3O_4 (1:1) NPs were found to be 19.04, 31.31, 36.89, 38.42, 44.86, 55.76, 59.39, 65.31 and 77.44, 78. 45 with the resulting miller indices value of 111, 220, 311, 222, 400, 422, 511, 440, 533 and 622, respectively. While the ≈ 2θ of Co_3O_4 (1:2) were estimated as 19.58, 31.26, 36.11, 38.68, 44.76, 55.65, 59.35, 65.21, 76.91 and 77.41 with its counterpart of miller indices vale of 111, 220, 311, 222, 400, 422, 511, 440, 533 and 622, respectively.

The XRD pattern of Co_3O_4 NPs was presented in Fig.4. All the peaks were cubic with space group Fd3m(227) and approximately close to the reported information (jcpds-42-1467). Due to the crystal symmetry and related face velocities, the common crystal habit of Co_3O_4 is cubic in shape. In addition to this, XRD result also indicates that the (311) plane was the preferred growth plane as (311) peak was the most intense. Furthermore, the diffraction pattern of the formed Co_3O_4 NPs is rigid and narrow and this implies that Co_3O_4 NPs has a good crystalline structure because of the existence of high amount of *Ehretia cymosa thonn* leaf peel extract used during the synthesis process as a stabilizing and a capping agent, which fits with the porosity of the green mediated synthesized Co_3O_4 NPs.

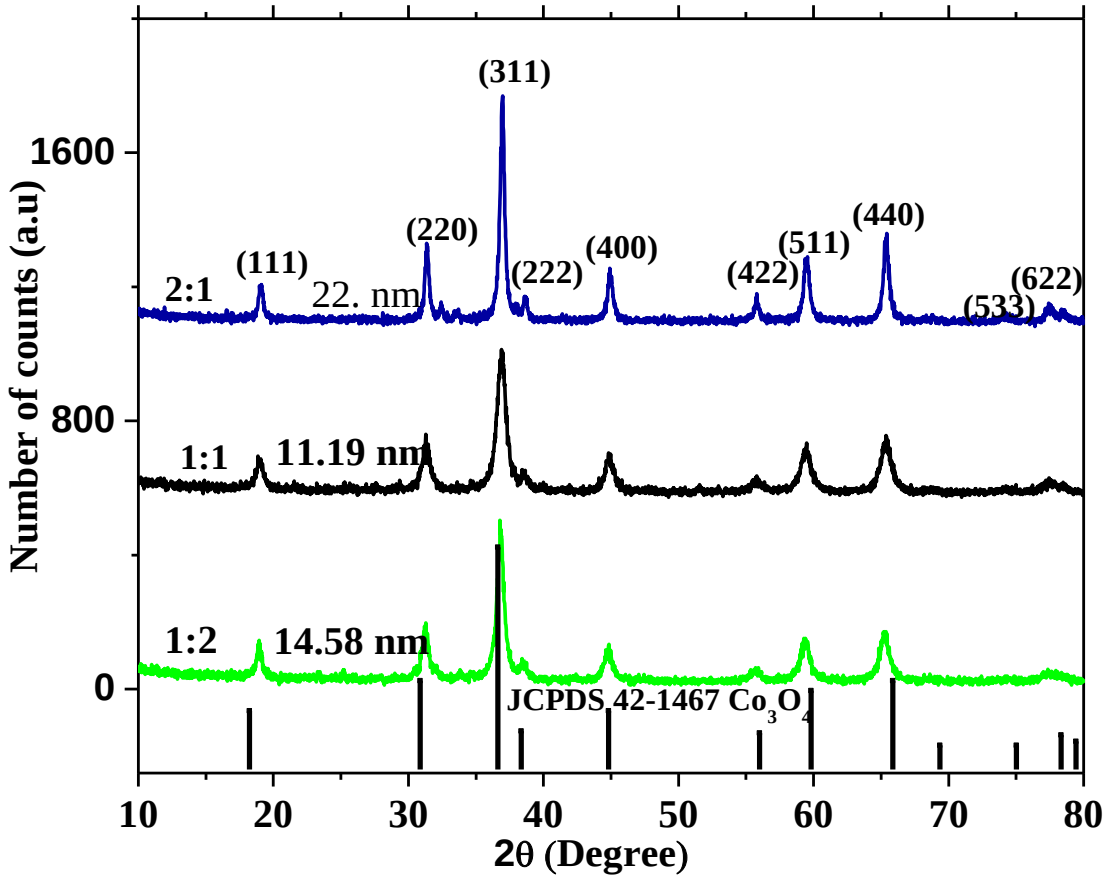

Figure 5. XRD spectra of *Ehretia cymosa thonn* mediated synthesized Co_3O_4 NPs

From Figure 3 and 4, the XRD analysis of both ZnO and Co_3O_4 NPs showed similar phenomenon. Furthermore, the analysis confirms that, the leaf of *Ehretia cymosa thonn* was played a great role to maintain more stable ZnO and Co_3O_4 NPs. It has found that in both of the NPs, the 1:1 volume ratios of ZnO and Co_3O_4 NPs possess smaller average crystalline size as compared to the counter parts.

4.2. SEM Analysis of ZnO and Co_3O_4 NPs

The surface morphologies of green synthesized ZnO nanoparticles within the ratio of 2:1, 1:1, and 1:2 were studied by using SEM, and the results are presented in Figure 5 (a, b, and c), respectively. The image showed that all the volume ratios of the synthesized ZnO NPs were spherical shapes, in which the particles are also found to be inclined together due to the presence of more capping agent that stabilizes the formed nanoparticles. The SEM analysis also confirms that the synthesized ZnO NPs has spherical shapes and a few particles are found to be fasten together. Figure 5a, proves the SEM image of the ZnO (2:1) and this analysis confirms as it was found to be relatively homogenized surface morphology relative to the

remaining ratios of ZnO. This could be due to the presence of excess volume of capping and reducing agent relative to the count parts that controls the overgrowth of ZnO and enables to have homogenized image.

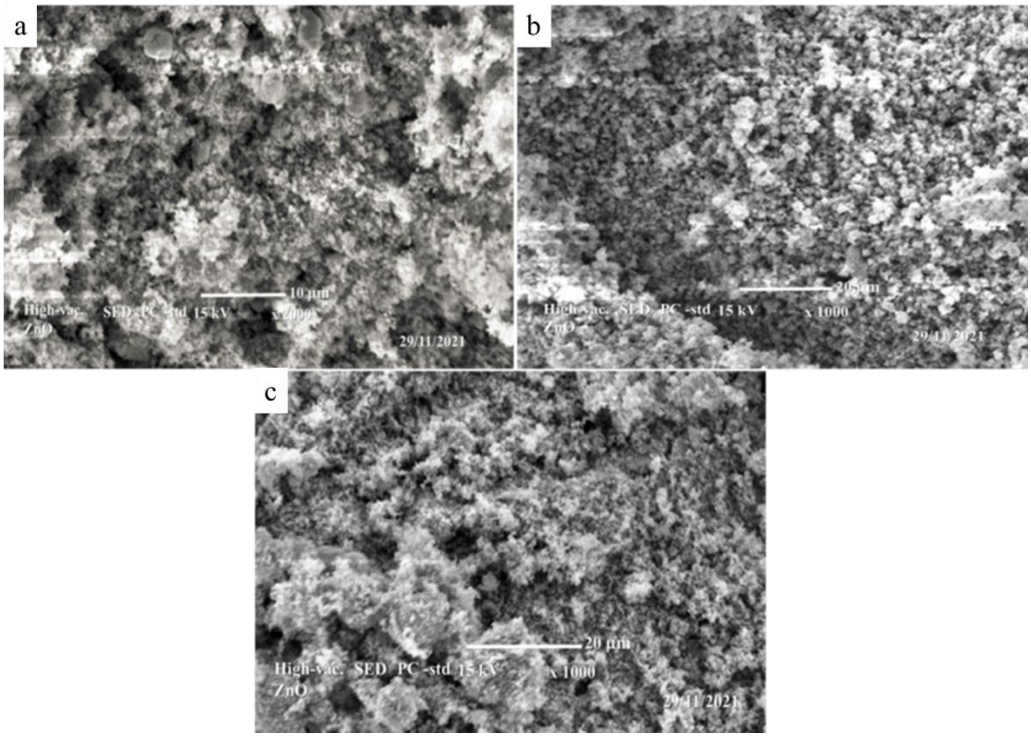

Figure 6. SEM image of ZnO NPs a) 2:1, b), 1:1, and c) 1:2 volume ratios, respectively.

The SEM analysis was found to be fit with the XRD analysis and these re-again tell us the formation of pure ZnO NPs. A homogenous distribution of particles can give us better knowledge on a morphological study and approximate particles size that fits with the XRD result of ZnO NPs.

In the same technique, the surface morphology of green synthesized Co_3O_4 nanoparticles formed within volume ratios of 1:1, 2:1, and 1:2 were viewed through the SEM under Figure 6 (a, b and c) for the 1:1, 2:1, and 1:2, respectively. Figure 6 shows the SEM images of *Ehretia cymosa thonn* leaf mediated synthesized cobalt oxide nanoparticles. The SEM image reveals the shape and morphology of the various volume ratios of Co_3O_4 nanoparticles were found to be spherical in shape. The image also elucidates the decrease of particle size as supported and confirmed from the XRD analysis, implies the well association of biomolecules obtained from the extract of *Ehretia cymosa thonn* leaf with that of Co_3O_4 precursor salt during the biosynthesis process and the presence of the extract coats the surface of Co_3O_4 NPs, thus preventing from aggregation and agglomeration and so results in a relatively homogenized surface morphology. Among the three volume ratios, the surface morphology of Co_3O_4 (1:1) are too homogenized

implies the well association of biomolecules obtained from the extract with Co_3O_4 nanoparticles during the synthesis process; and the presence of the extract coats the surface of the Co_3O_4 nanoparticles, thus preventing from aggregation. As it can be shown from Figure 6c, the particles show agglomeration which results due to the presence of excess amount of leaf extract of *Ehretia cymosa thonn*, which was beyond the coating surface of Co_3O_4 NPs.

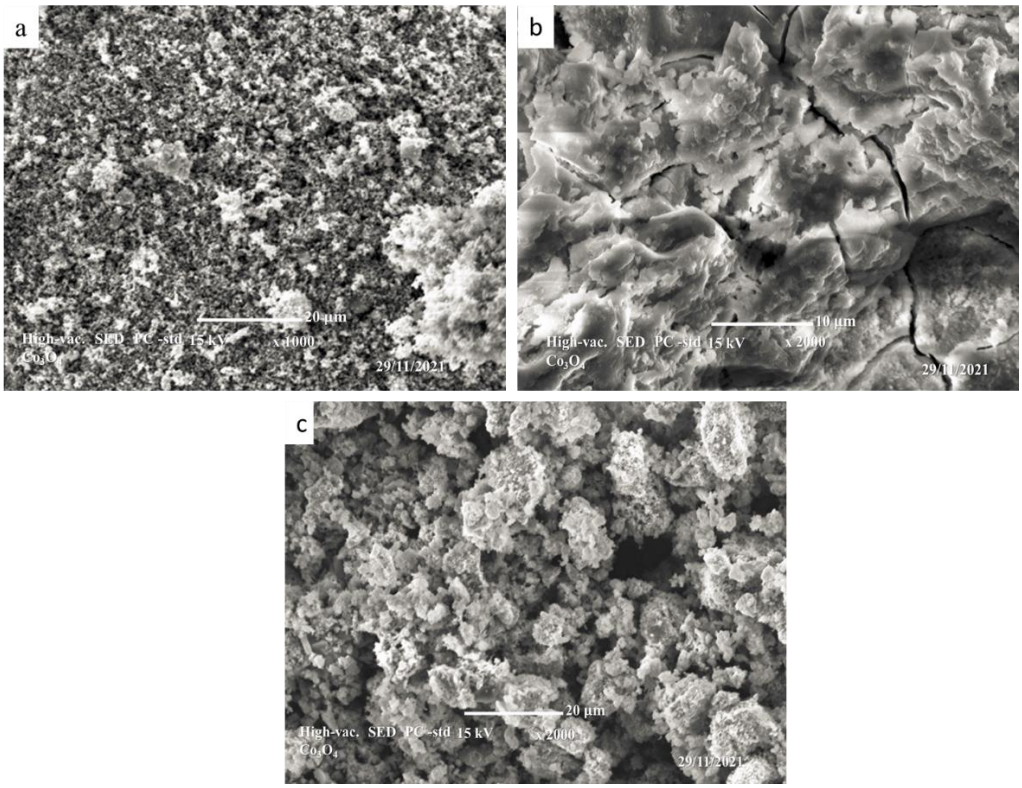

Figure 7. SEM micrograph of Co_3O_4 synthesized within a) 1:1, b) 2:1, and c) 1:2 volume ratios.

Moreover, it is clear from the SEM micrograph image that the particles are found to be highly crystalline. The characteristic of FCC Co_3O_4 NPs is observed, showing that the structure seen in the SEM image are nanocrystalline in nature due to the presence of the leaf extract of *Ehretia cymosa thonn* that acts as both reducing and capping agent. It is observed that the all volume ratios of Co_3O_4 nanoparticles are scattered over the surface and no aggregates are noticed under SEM as indicated under Figure 6.

4.3. UV-Vis Analysis of ZnO and Co_3O_4 NPs

The optical property of green achieved ZnO and Co_3O_4 NPs were characterized using UV-Vis characterization techniques. Figure 7 shows the UV-Vis absorption spectrum of green templated zinc oxide nanoparticles. Strong absorption bands of the sample were observed from UV-Vis spectra, which

correspond to the characteristic band of ZnO nanoparticles. The calculated energy band gap energy of the green obtained ZnO NPs was estimated as 3.34, 3.27, and 3.25 eV for the volume ratios of 1:1, 2:1, and 1:2, respectively, which is found to be fit with the previously related work. As can be depicted under Figure 7, oscillation of electrons in the conduction band at a particular wavelength around λ_{max} was due to the effect of surface plasmon resonance. The steady increase in the absorbance intensities of ZnO NPs in the UV-Vis spectra clearly indicates the increased formation of ZnO NPs.

The bioactive phytochemicals present in the leaf extract of *Ehretia cymosa thonn* reduces Zn^{2+} ions to zero valent Zn atoms initially during the synthesis process. These zero valent Zn atoms initiates the nucleation and involved in the reduction of residual Zn^{2+} to ZnO and its further growth leads to cluster formation and production. Moreover, the spectrum revealed a strong peak located around at 379 nm, which was the characteristic peak of green synthesized zinc oxide NPs. ZnO NPs were highly nano-sized and the emergence of absorption peak was owing to surface plasmon resonance phenomena. Generally the UV-Vis analyses of the various volume ratios of ZnO NPs were found to fit with its corresponding XRD average crystalline size. Since ZnO NPs with relatively smaller average crystalline size should have relatively large bad gap energy, which is also the case in the present findings too. As can be presented within Figure 7, the peaks have changed with the variation in volume ratios. This might again results in the change of optical property of the synthesized NPs. Since, as the extract is added, the conductivity and the light absorption behavior also changed.

The optical absorption properties have been verified by measuring the UV-Vis spectroscopy of the green synthesized Co_3O_4 NPs synthesized within the ratios of 1:1, 2:1, and 1:2 depicted under Figure 8. The Figure shows the UV-Vis absorption spectrum of the green synthesized Co_3O_4 NPs, which presents two absorption bands in the wavelength ranges of 200-290 and 330-370 nm. The appearance of first band near UV region is ascribed to the $O^{2-} \rightarrow Co^{2+}$ charge transfer process, and the second absorption band near green region is attributed to the $O^{2-} \rightarrow Co^{3+}$ charge transfer, confirming the formation of Co_3O_4 NPs. Green synthesized Co_3O_4 NPs shows absorption dominantly in the UV region and partially in the visible region of the spectrum. The band gap energy of *Ehretia cymosa thonn* leaf mediated green synthesized Co_3O_4 NPs within the volume ratios of 1:1, 2:1, and 1:2 were was estimated using the equation $E_g = \frac{hc}{\lambda}$, where h is planks constant, c is speed of light and λ is the wavelength at which maximum absorption is occurred and is found from the UV-Vis absorption spectrum of green synthesized cobalt oxide NPs. The calculated band gap energy of Co_3O_4 NPs was found to be 3.77, 3.70, and 3.55 eV for the volume ratios of 1:1, 1:2, and 2:1, respectively. It has been found that, the UV-Vis absorption spectra of the green synthesized Co_3O_4 NPs were found to fit with both XRD and the SEM analysis. Co_3O_4 NPs with smaller average crystalline size

possess relatively homogenized surface morphology and large band gap energy. This analysis was found to be related with the previously reported work.

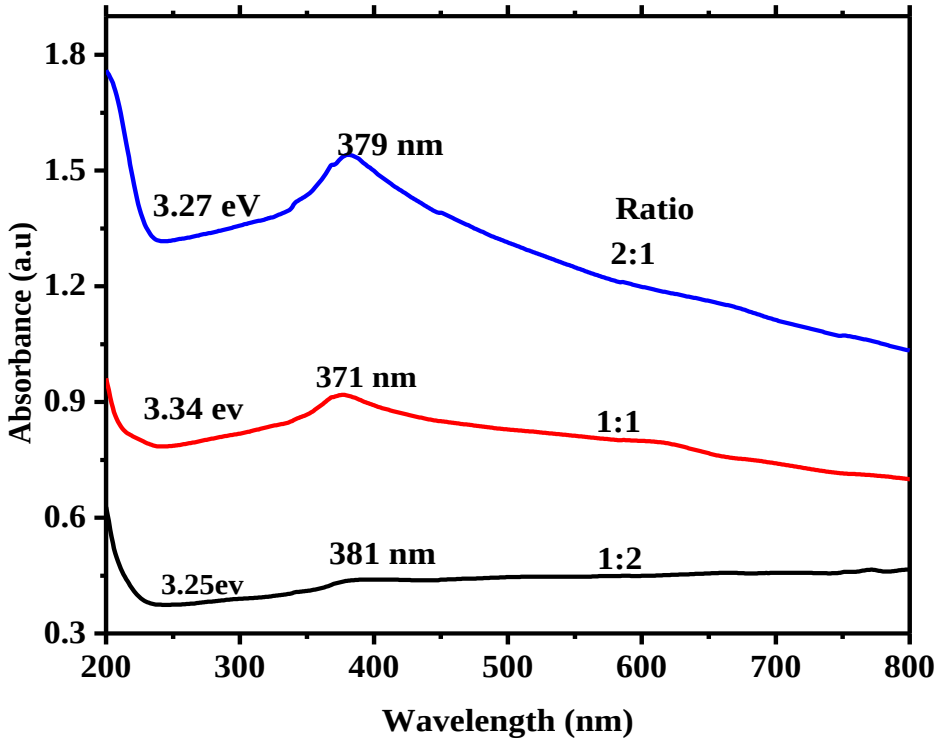

Figure 8. UV-Vis absorption spectra of green synthesized ZnO NPs.

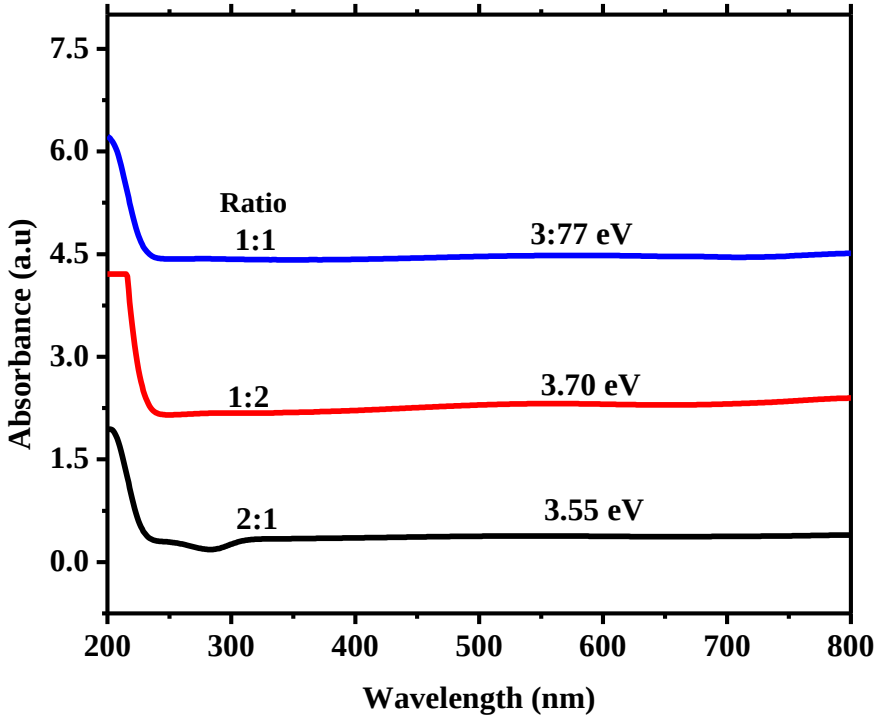

Figure 9. UV-Vis absorption spectra of green synthesized Co_3O_4 NPs.

Therefore, it can be conclude that the optical behavior of green obtained cobalt oxide NPs were found to be fit with the XRD result, since as the average crystalline size of green mediated synthesized cobalt oxide NPs becomes small the band gap energy becomes large. Moreover, green synthesized cobalt oxide NPs possess high band gap energy as compared to chemically formed cobalt oxide NPs due to the smaller average crystalline size as can be found from the XRD spectrum.

4.4. FT-IR Analysis of ZnO and Co_3O_4 NPs

Fourier transformation infrared (FTIR) spectroscopy analysis technique was done to identify and confirm the role of biomolecules of *Ehretia cymosa thonn* leaf that was responsible for capping and reducing during the synthesis of ZnO NPs. Figure 9 displays both the FT-IR spectra of the leaf powder of *Ehretia cymosa thonn* and the formed ZnO NPs. It has been found that in the case of ZnO NPs, the peaks are located at around 3421.06, 2920.48, 1623.46, 1313.19, and 478.30 cm^{-1}.

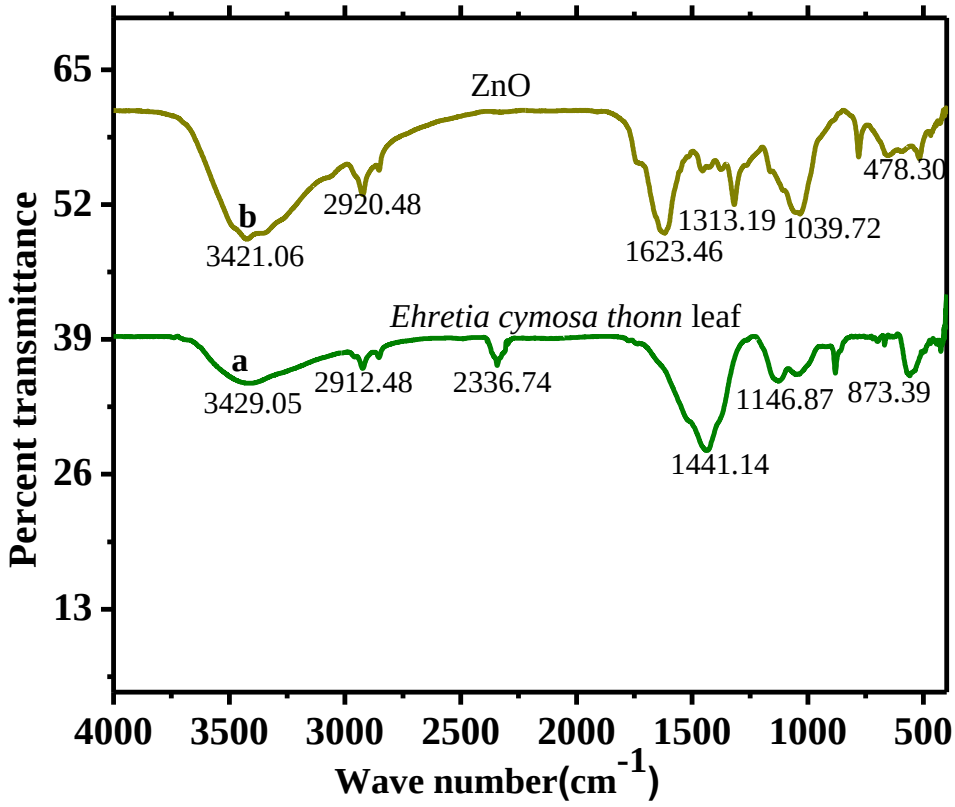

Figure 10. FT-IR spectra of ZnO and leaf powder of *Ehretia cymosa thonn*.

The wide broad absorption peak observed at 3421.06 cm^{-1} represents the presence of Zn-OH bonds and the alkane (C-H) bond in stretching mode was identified by the peaks observed at 2920.48 cm^{-1}. This peak may also attribute to the asymmetric and symmetric stretching vibrations of $-CH_2$ groups. The medium absorption peak found at 1623.46 cm^{-1} represents the C=O stretching of primary amide or to C=C groups of

aromatic rings that plays as stabilizer and reducing agents during the stage of synthesis. This band also relates to the bending mode of vibration of O-H group and flavones found within the leaf extract. The 1313.19 cm^{-1} represents carbon dioxide and/or due to O-H bending of molecularly adsorbed water on the surface of the synthesized material. The formation of Zn-O stretching vibration were found at around 478.30 cm^{-1} and this represents and confirms as ZnO NPs were synthesized via a green method using leaf extract of *Ehretia cymosa thonn*.

In order to check and confirm the role of leaf extract of *Ehretia cymosa thonn* during the synthesis of ZnO as both a capping and reducing agent, the powder were also allowed for FT-IR characterization and the peaks were found to be located at 3429.05, 2912.48, 2336.78, 1441.14, 1146.87 and 873.39 cm^{-1}. The broad absorption band observed at 3429.05 cm^{-1} represents O-H bond stretching due to adsorbed moisture on the surface of the green synthesized ZnO NPs, and the weak absorption band at 2912.48 cm^{-1} is due to C=O bond stretching that could be emanated from the presence of adsorbed carbon dioxide on the surface of NPs. The weak absorption peak found around 2336.78 cm^{-1} refers to C=O bond stretching that might be due to the presence of adsorbed carbon dioxide on the surface of green mediated ZnO NPs as well as the surface water and hydroxyl groups and the C-H of alkenes. While 1441.14 cm^{-1} reveals C-C stretching is linked with polyphenols & natural pigment of the leaf extract. The peak found in the range of 1146.87 and 873.39 cm^{-1} indicated the presence of C-O-H bending mode of vibration and as well this peak present in ZnO signified amide band of the random coil of protein. By nature FT-IR characterization is an intensive and independent and doesn't vary with the variation in volume ratios between the crude extract and the precursor salt, so under this study only one ratio of ZnO was done.

The functional groups that could cap the surface of the cobalt oxide nanoparticles were confirmed by using FT-IR studies. Figure 10a and 10b represents the FT-IR spectrum of green synthesized cobalt oxide NPs formed within the volume ratios of 2:1 and powder of *Ehretia cymosa thonn*, respectively. As indicated in Figure 10a, the O-H stretch appears in the spectrum as a very broad band extending from 3420.4 cm^{-1}. This very broad O-H stretched band is observed with a C=O peak, which is almost, certainly indicates that the compound is an aliphatic carboxylic acid. Prominent levels of absorption were observed at 2925.2 and 2315.0 cm^{-1} reveal the presence of C-H stretching vibrations of an aromatic aldehyde and amide (C≡N) functional groups, respectively.

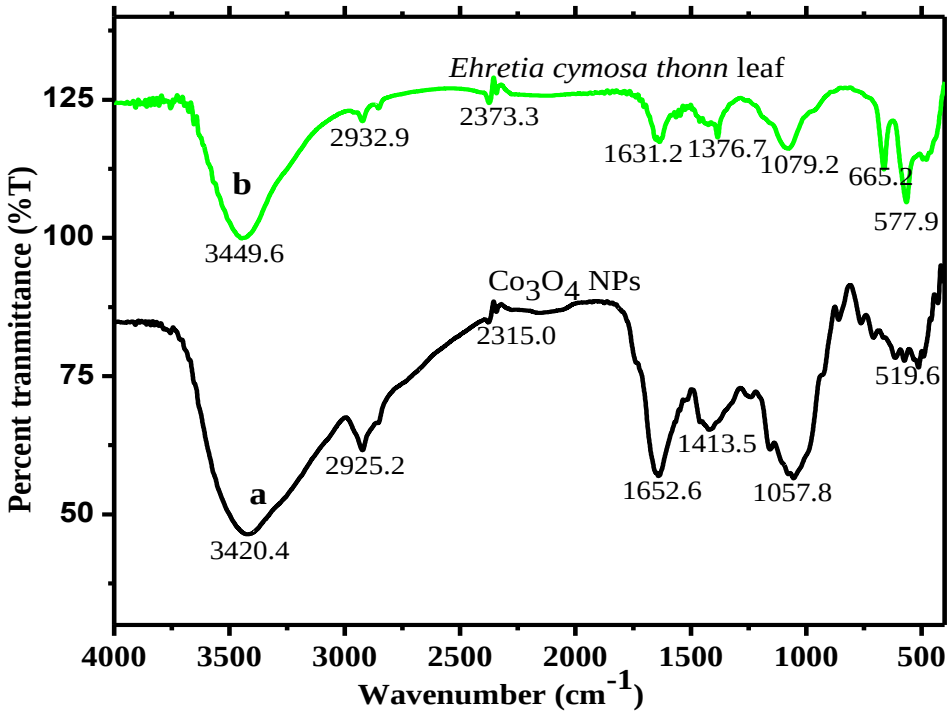

Figure 11. FT-IR spectra of Co_3O_4 (1:1) NPS and extract of *Ehretia cymosa thonn* leaf.

In addition to this, the peak observed at 1652.6 and 1413.5 cm^{-1} corresponds to C=O peak, which indicates ketone as well ammine functional groups and carbonyl group of flavonoids, respectively. An absorption peak found at 1057.8 cm^{-1} corresponds to saturated primary alcohol C-O stretching. The FT-IR spectrum of cobalt oxide (Co-O) nanoparticles absorbs at 519.6 cm^{-1}, which was matched with the results reported previously. Thus, it can be observed from the FT-IR spectrum that Co_3O_4 NPS is significantly rich in different chemical groups such as primary alcohols, alkanes, carboxylic acids, flavonoids, amide, aldehydes and ketones.

Figure 10b indicates absorption bands of *Ehretia cymosa thonn* leaf extract. Strong absorption peaks located at 3449.6 cm^{-1} for O-H band stretching mode, which are phenols and alcohols. The absorption at 2932.9 cm^{-1} is aromatic of C-H band and primary ammine stretching mode. The absorption at 2374.3 cm^{-} indicates amide (C≡N). The absorption at 1631.2 cm^{-1} can be assigned to the aromatic C=C mode of stretching. The peak observed at 1376.7 cm^{-1} indicates the presence of flavonoid within the extract of *Ehretia cymosa thonn* leaf. Furthermore, the absorption band found in the range of around 1079.2-577.9 cm^{-1} shows the stretching mode of C-O. In Figure 10a, the absence of functional groups around 660 cm^{-1} indicates that, this functional group was removed during the process of calcination. Since, this characterization technique is intensive (independent of amount), so, characterizing the individual ratios don't alter the nature of the functional groups and as well the formation of Co-O bonding.

4.5. Antibacterial Activities of ZnO and Co_3O_4 NPs

The antibacterial activity of green synthesized ZnO NPs was investigated against selected both Gram negative and Gram positive pathogens of *S. Aureus* and *Escherichia coli* via disk diffusion method within three different concentrations of ZnO (50, 75 and 100 µg/mL). It has been found that as the concentration of ZnO-NPs increases, the zone of inhibition also increased against the bacteria strains. As can be confirmed from the zone of inhibition both from the table and the image, Zinc oxide nanoparticles have a significant growth inhibition effect against *S. Aureus and E. coli bacteria*. This effect is resulted from high surface area of ZnO NPs and their small average crystalline size. Figure 11 displays the image of zone of inhibition of ZnO NPs at various concentrations against *S. Aureus* and *E. coli*. In both Gram negative and Gram positive bacteria species, as the concentration increases, the zone of inhibition (ZOI) also improved and this in turn confirms and proves the effect of concentration on antibacterial treatment. Gram +ve bacteria show significant ZOI than negative bacteria due to more reactive oxygen species in Gram negative bacteria.

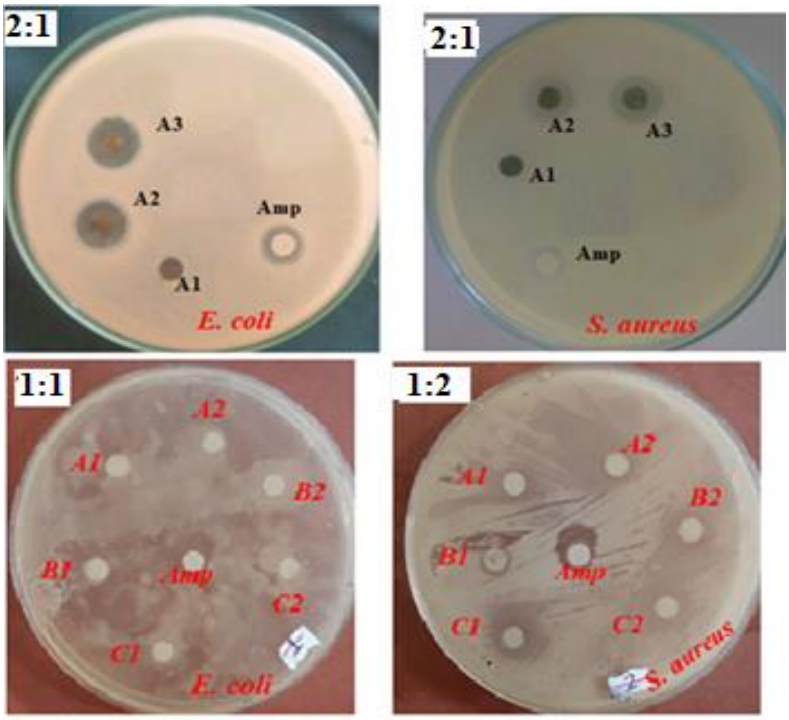

Figure 12. Antibacterial activity of ZnO NPs at different concentrations (50, 75 and 100 µg/mL).

Table 1. Summarizes the ZOI of the synthesized ZnO NPs against the two bacteria pathogens.

Concentration and ratio	Bacteria Species and Zone of Inhibition in (mm)	
	E. coli ATCC25922	*S. aureus* ATCC25923
1:1		
A1 (50 µg/mL)	8	9
B1 (75 µg/mL)	15	13
C1 (100 µg/mL)	18	16
2:1		
A1 (50 µg/mL)	9	10
A2 (75 µg/mL)	10	13
A3 (100 µg/mL	12.5	16
1:2		
A1 (50 µg/mL)	8	8
B1 (75 µg/mL)	9	10
C1 (100 µg/mL	11	11.5
Ampicillin (standard)	13	14

As can be presented under table 1, the antibacterial activity of green synthesized ZnO showed improved potential even as compared to the standard (ampicillin). This proves that, green synthesized ZnO NPs could be applied and used within health centers and in different food beverages instead of using commercially synthesized and too costy antibiotics. It has been found that ZnO NPs within 1:1 ratios showed the best antibacterial activity relative to the counter parts. This is due to the fact that ZnO 1:1) possess the smallest average crystalline sized from the XRD result and homogenized surface morphology from the SEM image. This confirms that ZnO NPs with smaller average crystalline size and homogenized surface morphology can have high antibacterial activity, since smaller size implies high surface area and so enhanced antibacterial activity.

The antibacterial activity of the synthesized Co_3O_4 nanoparticles with the volume ratio of 1:2, 1:1, and 2:1 were investigated on both gram negative and gram-positive bacteria strains using disc diffusion method. To analyze the effect of nanoparticles concentration on antibacterial activity, 50, 75, and 100 µg/mL were prepared from green synthesized Co_3O_4 nanoparticles and tested using *E. coli* and *S. Aureus* bacteria *strains*. The antibacterial activity of each volume ratio of Co_3O_4 nanoparticles was compared with the positive control ampicillin; the results of antibacterial studies clearly suggests that, Co_3O_4 (2:1) nanoparticles synthesized through biological method shows better antibacterial activity at high concentration as compared to the other ratios. This is due to the fact that, the average crystalline size of this

cobalt oxide is smaller than the other ratios. Furthermore, in green synthesized Co_3O_4 nanoparticles produce high amount of reduced reactive oxygen species (ROS) due to the presence of the *Ehretia cymosa thonn* leaf extract. It has been observed that green synthesized cobalt oxide possessed antibacterial activity even as compared to the stand at enhanced concentrations. This analysis confirms that it could be preferable and cost effective to use green mediated synthesized cobalt oxide NPs instead of using commercially and too costy antibiotic drugs for the treatment of different aliments. The antibacterial activity analysis has established that the green synthesized Co_3O_4 NPs displayed outstanding antagonistic effects on both Gram positive and Gram-negative bacterial strains compared to the standard ampicillin, and the respective diameter of the inhibition zones in the bacterial strains are due to the antibacterial potential of the Co_3O_4 NPs. As it were reported previously, the differences in the susceptibility of different bacterial strains are due to the differences in their oxidative stress tolerance. Figure 12 shows the zone of inhibition of the synthesized Co_3O_4 nanoparticles against the two bacteria strains.

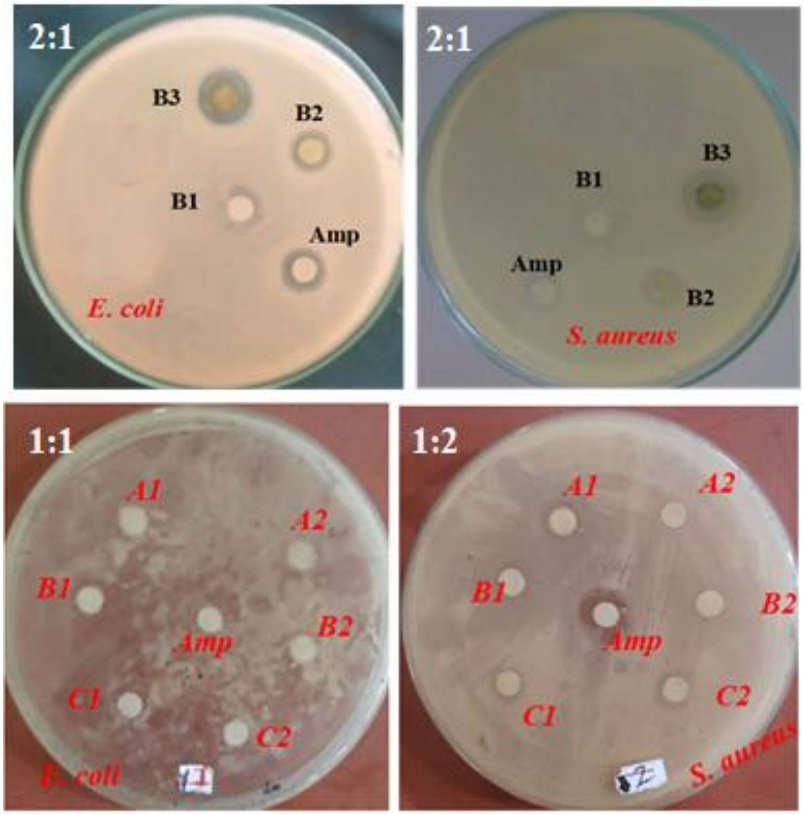

Figure 13. Antibacterial activity of Co_3O_4 NPs at various concentrations (50, 75 and 100 µg/mL) against *A. Aureus* and *E. coli*.

Furthermore, the antibacterial potential of Co_3O_4 NPs is due to the result of an electrostatic interaction between the bacterial cell and the nanoparticles, which are capable of generating reactive oxygen species (ROS), a factor responsible for the bacterial cell destruction is due to the result of an electrostatic interaction between the bacterial cell and the nanoparticles. From the image of zone of inhibition and the

table, it has been observed that, Co_3O_4 (2:1) NPs found to be the most promising antibacterial drug. Again Co_3O_4 (1:2) NPs also proves better antibacterial activity next to the 2:1 ratios and this might be contributed due to the existence of the high amount of extract that results in the prodcution of excess ROS. Similarlly, the 1:1 ratios also shows better antibacterial activity and from this analysis, it could be found that, Co_3O_4 NPs synthesized in the three different volume ratios found to be a promising antibacterial drug; which could be easily synthesized at the laboratory level using environmentally available starting materials.

Table 2. Showed the summery of effect of volume and concetration of Co_3O_4 NPs on the antibacterial activity.

Ratio & concentration	Bacteria Species and Zone of Inhibition (mm)	
	E. coli ATCC25922	*S. Aureus* ATCC25923
2:1		
B1 (50µg/mL)	7	7
B2 (75µg/mL)	13	12
B3 (100µg/mL)	16	15
1:1		
A1 (50 µg/mL)	8	9
B1 (75 µg/mL)	9	10
C1 (100µg/mL)	10	11
1:2		
A2 (50 µg/mL)	9	9
B2 (75 µg/mL)	11	11
C3 (100µg/mL)	12	13

4.6. Comparative Study of Co_3O_4 and ZnO Nanoparticles

From the present findings, it can be summarized that both of the green synthesized NPs showed improved antibacterial activity. The study promised that instead of using commercially synthesized and too costy antibiotics available at different pharmacies and hospitals, it could be most preferable to use environmentally friendly synthesized NPs as effective antibiotics. Both of the NPs synthesized within various volume ratios were found to be effective in treating both Gram negative and Gram positive bacteria causing disease. In addition to this as the concentration of the drug is improved, the effectiveness also increased. However, the antibacterial activity of green synthesized ZnO NPs found to be more effective as compared to the green synthesized various volume ratios of Co_3O_4 NPs. This enhanced antibacterial activity might be contributed from the smaller average crystalline size of ZnO NPs. Since as the average crystalline size of ZnO NPs is becomes too small, the surface area also increased, which enables in killing

more bacterial cells. Furthermore, the enhanced antibacterial activity of green synthesized ZnO NPs results from the more homogenized and uniform morphology as compared to the counter parts.

5. Conclusion

In the present findings, ZnO and Co_3O_4 NPs were succsesfully synthesized in the presence of leaf extract of *Ehretia cymosa thonn* as green alternative method. The formation of stable and green ZnO and Co_3O_4 NPs were characterized via XRD, SEM, FTIR and UV-Vis spectroscopic techinques. At the end, the antibacterial activity of those green synthesized NPs were investigated against *E.coli* and *S.Aures.* The effect of volume ratios and variotion of concentration of the syntheszied antibiotic drug were well investigated. The XRD analysis proves the formation of pure and highly stable ZnO and Co_3O_4 NPs without the formation of secondary phase, which intern confirms the formation of pure and highly crystalline NPs. In both of the NPs, the XRD analysis depicts as the 1:1 volume ratios were found to posses the smaller average cystalline size as compared to the counter parts. Moreover, the SEM findings indicates that both of the green synthesized ZnO and Co_3O_4 NPs have spherical in shape with some aggregation, which occurred due to the variation in the volume ratios of the precursors salt and the leaf extract of *Ehretia cymosa thonn*. In addition, the optical property of these green synthesized NPs was analyzed via UV-Vis spectroscopy. The calculated band gap energy of ZnO NPs formed with various volume ratios were found to in the range of 3.25-3.34 eV. While the band gap energy of Co_3O_4 NPs were found in the range of 3.55-3.77 eV. The FT-IR analysis showed the interaction between the extract with ZnO and Co_3O_4 NPs and the analysis proved as it contains several bioactive molecules such as flavonoid, ketone, carboxylic acid, and alcohol, saturated and unsaturated hydrocarbons. The presence of these functional groups enables to obtain stable and green alternative antibiotic drug with minimum cost and easy method of fabrication. As shown in the result part of this work, the study assured that ZnO NPs is more efficient than Co_3O_4 NPs in inhibiting bacterial pathogens.

References

Abebe, B., Zereffa, E. A., Tadesse, A., & Murthy, H. C. A. (2020). A Review on Enhancing the Antibacterial Activity of ZnO: Mechanisms and Microscopic Investigation. *Nanoscale Research Letters*, *15*(1). https://doi.org/10.1186/s11671-020-03418-6

Ahmad, S., Munir, S., Zeb, N., Ullah, A., Khan, B., Ali, J., Bilal, M., Omer, M., Alamzeb, M., Salman, S. M., & Ali, S. (2019). Green nanotechnology: A review on green synthesis of silver nanoparticles — An ecofriendly approach. *International Journal of Nanomedicine*, *14*, 5087–5107. https://doi.org/10.2147/IJN.S200254

Annu, Ali, A., & Ahmed, S. (2018). Green Synthesis of Metal, Metal Oxide Nanoparticles, and Their Various Applications. *Handbook of Ecomaterials*, 1–45. https://doi.org/10.1007/978-3-319-48281-1_115-1

Asamoah, R. B., Annan, E., Mensah, B., Nbelayim, P., Apalangya, V., Onwona-Agyeman, B., & Yaya, A. (2020). A Comparative Study of Antibacterial Activity of CuO/Ag and ZnO/Ag Nanocomposites. *Advances in Materials Science and Engineering*, *2020*. https://doi.org/10.1155/2020/7814324

Benhammada, A., & Trache, D. (2021). Green synthesis of CuO nanoparticles using Malva sylvestris leaf extract with different copper precursors and their effect on nitrocellulose thermal behavior. *Journal of Thermal Analysis and Calorimetry*, *0123456789*. https://doi.org/10.1007/s10973-020-10469-5

Bibi, I., Nazar, N., Iqbal, M., Kamal, S., Nawaz, H., Nouren, S., Safa, Y., Jilani, K., Sultan, M., Ata, S., Rehman, F., & Abbas, M. (2017). Green and eco-friendly synthesis of cobalt-oxide nanoparticle: Characterization and photo-catalytic activity. *Advanced Powder Technology*, *28*(9), 2035–2043. https://doi.org/10.1016/j.apt.2017.05.008

Chen, J. S., Zhu, T., Hu, Q. H., Gao, J., Su, F., Qiao, S. Z., & Lou, X. W. (2010). Shape-controlled synthesis of cobalt-based nanocubes, nanodiscs, and nanoflowers and their comparative lithium-storage properties. *ACS Applied Materials and Interfaces*, *2*(12), 3628–3635. https://doi.org/10.1021/am100787w

Choi, S., & Choy, J. (2014). *Biokinetics of zinc oxide nanoparticles : toxicokinetics , biological fates , and protein interaction*. 261–269.

Demissie, M. G., Sabir, F. K., Edossa, G. D., & Gonfa, B. A. (2020). *Synthesis of Zinc Oxide Nanoparticles Using Leaf Extract of Lippia adoensis (Koseret) and Evaluation of Its Antibacterial Activity*. *2020*.

Dewi, N. O. M., Yulizar, Y., & Bagus Apriandanu, D. O. (2019). Green synthesis of Co3O4 nanoparticles using Euphorbia heterophylla L. leaves extract: Characterization and photocatalytic activity. *IOP Conference Series: Materials Science and Engineering*, *509*(1). https://doi.org/10.1088/1757-899X/509/1/012105

Dobrucka, R., & Długaszewska, J. (2016). Biosynthesis and antibacterial activity of ZnO nanoparticles using Trifolium pratense flower extract. *Saudi Journal of Biological Sciences*, *23*(4), 517–523. https://doi.org/10.1016/j.sjbs.2015.05.016

Ghosh, M. K., Sahu, S., Gupta, I., & Ghorai, T. K. (2020). Green synthesis of copper nanoparticles from an extract ofJatropha curcasleaves: characterization, optical properties, CT-DNA binding and photocatalytic activity. *RSC Advances*, *10*(37), 22027–22035. https://doi.org/10.1039/d0ra03186k

Hafeez, M., Shaheen, R., Akram, B., Zain-Ul-Abdin, Haq, S., Mahsud, S., Ali, S., & Khan, R. T. (2020). Green synthesis of cobalt oxide nanoparticles for potential biological applications. *Materials Research Express*, *7*(2). https://doi.org/10.1088/2053-1591/ab70dd

Happy, A., Soumya, M., Kumar, S. V., Rajeshkumar, S., Sheba, R. D., Lakshmi, T., & Nallaswamy, V. D. (2019). Phyto-assisted synthesis of zinc oxide nanoparticles using Cassia alata and its antibacterial activity against Escherichia coli. *Biochemistry and Biophysics Reports*, *17*(September 2018), 208–211. https://doi.org/10.1016/j.bbrep.2019.01.002

Huang, X., Cai, H., Zhou, H., Li, T., Jin, H., Evans, C. E., Cai, J., & Pi, J. (2021). Cobalt oxide nanoparticle-synergized protein degradation and phototherapy for enhanced anticancer therapeutics. *Acta Biomaterialia*, *121*, 605–620. https://doi.org/10.1016/j.actbio.2020.11.036

Hussain, I., Singh, N. B., Singh, A., Singh, H., & Singh, S. C. (2016). Green synthesis of nanoparticles and its potential application Green synthesis of nanoparticles and its potential application. *Biotechnology Letters*, *38*(4), 545–560. https://doi.org/10.1007/s10529-015-2026-7

Jamdagni, P., Khatri, P., & Rana, J. S. (2018). Green synthesis of zinc oxide nanoparticles using flower extract of Nyctanthes arbor-tristis and their antifungal activity. *Journal of King Saud University - Science*, *30*(2), 168–175. https://doi.org/10.1016/j.jksus.2016.10.002

Jia, H., Yang, D., Han, X., Cai, J., Liu, H., & He, W. (2016). Peroxidase-like activity of the Co3O4 nanoparticles used for biodetection and evaluation of antioxidant behavior. *Nanoscale*, *8*(11), 5938–5945. https://doi.org/10.1039/c6nr00860g

Jiang, J., Pi, J., & Cai, J. (2018). *The Advancing of Zinc Oxide Nanoparticles for Biomedical Applications*. *2018*. https://doi.org/10.1155/2018/1062562

Kalpana, V. N., & Devi Rajeswari, V. (2018). A Review on Green Synthesis, Biomedical Applications, and Toxicity Studies of ZnO NPs. *Bioinorganic Chemistry and Applications*, *2018*. https://doi.org/10.1155/2018/3569758

Kiani, M., Rabiee, N., Bagherzadeh, M., Ghadiri, A. M., Fatahi, Y., Dinarvand, R., & Webster, T. J. (2021). Improved green biosynthesis of chitosan decorated Ag- and Co3O4-nanoparticles: A relationship between surface morphology, photocatalytic and biomedical applications. *Nanomedicine: Nanotechnology, Biology, and Medicine*, *32*, 102331. https://doi.org/10.1016/j.nano.2020.102331

Kolodziejczak-Radzimska, A., & Jesionowski, T. (2014). Zinc oxide-from synthesis to application: A review. *Materials*, *7*(4), 2833–2881. https://doi.org/10.3390/ma7042833

Matinise, N., Mayedwa, N., Fuku, X. G., Mongwaketsi, N., & Maaza, M. (2018). Green synthesis of cobalt (II, III) oxide nanoparticles using Moringa Oleifera natural extract as high electrochemical electrode for supercapacitors. *AIP Conference Proceedings*, *1962*. https://doi.org/10.1063/1.5035543

Mittal, A. K., Chisti, Y., & Banerjee, U. C. (2013). Synthesis of metallic nanoparticles using plant extracts. *Biotechnology Advances*, *31*(2), 346–356. https://doi.org/10.1016/j.biotechadv.2013.01.003

Nasrollahzadeh, M., Momeni, S. S., & Sajadi, S. M. (2017). Green synthesis of copper nanoparticles using Plantago asiatica leaf extract and their application for the cyanation of aldehydes using K 4 Fe(CN) 6. *Journal of Colloid and Interface Science*, *506*, 471–477. https://doi.org/10.1016/j.jcis.2017.07.072

Navarro-Yepes, J., Burns, M., Anandhan, A., Khalimonchuk, O., Del Razo, L. M., Quintanilla-Vega, B., Pappa, A., Panayiotidis, M. I., & Franco, R. (2014). Oxidative stress, redox signaling, and autophagy: Cell death versus survival. *Antioxidants and Redox Signaling*, *21*(1), 66–85. https://doi.org/10.1089/ars.2014.5837

Ogundajo, A., Nnaemeka, C., Olawunmi, R., & Ogunwande, siaka. (2016). Chemical Constituents of Essential Oil of Ehretia cymosa Thonn. *British Journal of Applied Science & Technology*, *14*(4), 1–6. https://doi.org/10.9734/bjast/2016/24240

Pagar, T., Ghotekar, S. K., & Pansambal, S. (2019). A review on bio-synthesized Co3O4 nanoparticles using plant extracts and their diverse applications. *Journal of Chemical Reviews*, *1*(4), 260–270. https://doi.org/10.33945/sami/jcr.2019.4.2

Pavan Kumar, M. A., Suresh, D., Nagabhushana, H., & Sharma, S. C. (2015). Beta vulgaris aided green synthesis of ZnO nanoparticles and their luminescence, photocatalytic and antioxidant properties. *European Physical Journal Plus*, *130*(6). https://doi.org/10.1140/epjp/i2015-15109-2

Raeisi, M., Alijani, H. Q., Peydayesh, M., Khatami, M., Bagheri Baravati, F., Borhani, F., Šlouf, M., & Soltaninezhad, S. (2021). Magnetic cobalt oxide nanosheets: green synthesis and in vitro cytotoxicity. *Bioprocess and Biosystems Engineering*, *44*(7), 1423–1432. https://doi.org/10.1007/s00449-021-02518-6

Rasmussen, J. W., Martinez, E., Louka, P., & Wingett, D. G. (2010). *Zinc oxide nanoparticles for selective destruction of tumor cells and potential for drug delivery applications*. 1063–1077.

Ren, G., Hu, D., Cheng, E. W. C., Vargas-Reus, M. A., Reip, P., & Allaker, R. P. (2009). Characterisation of copper oxide nanoparticles for antimicrobial applications. *International Journal of Antimicrobial Agents*, *33*(6), 587–590. https://doi.org/10.1016/j.ijantimicag.2008.12.004

Rice, K. M., Ginjupalli, G. K., Manne, N. D. P. K., Jones, C. B., & Blough, E. R. (2019). A review of the antimicrobial potential of precious metal derived nanoparticle constructs. *Nanotechnology*, *30*(37). https://doi.org/10.1088/1361-6528/ab0d38

Rutberg, F. G., Dubina, M. V., Kolikov, V. A., Moiseenko, F. V., Ignat'eva, E. V., Volkov, N. M., Snetov, V. N., & Stogov, A. Y. (2008). Effect of silver oxide nanoparticles on tumor growth in vivo. *Doklady Biochemistry and Biophysics*, *421*(1), 191–193. https://doi.org/10.1134/S1607672908040078

Samy, A., El-Sherbiny, A. E., & Menazea, A. E. R. A. (2019). Green synthesis of high impact zinc oxide nanoparticles. *Egyptian Journal of Chemistry*, *62*, 29–37. https://doi.org/10.21608/EJCHEM.2019.12863.1802

Santhoshkumar, M., & Balupillai, A. (n.d.). *Biological Fabrication and Characterization of Zinc Oxide Nanoparticles Using Gymnema Sylvestre Potentially Produces Toxicity in Breast Cancer Cells*. 1–11.

Sarkodie, J. A., N'Guessan, B. B., Kretchy, I. A., & Nyarko, A. K. (2015). The antihyperglycemic , antioxidant and antimicrobial activities of Ehretia Cymosa. *Journal of Pharmacognosy and Phytochemistry*, *4*(3), 105–111. https://www.researchgate.net/publication/282155624_The_antihyperglycemic_antioxidant_and_antimicrobial_activities_of_Ehretia_Cymosa

Senthilkumar, N., Nandhakumar, E., Priya, P., Soni, D., Vimalan, M., & Vetha Potheher, I. (2017).

Synthesis of ZnO nanoparticles using leaf extract of: Tectona grandis (L.) and their anti-bacterial, anti-arthritic, anti-oxidant and in vitro cytotoxicity activities. *New Journal of Chemistry*, *41*(18), 10347–10356. https://doi.org/10.1039/c7nj02664a

Siddiqi, K. S., & Husen, A. (2016). Fabrication of Metal and Metal Oxide Nanoparticles by Algae and their Toxic Effects. *Nanoscale Research Letters*, *11*(1). https://doi.org/10.1186/s11671-016-1580-9

Siddiqi, K. S., Rahman, A., & Husen, A. (2018). *Properties of Zinc Oxide Nanoparticles and Their Activity Against Microbes*.

Singh, J., Dutta, T., Kim, K. H., Rawat, M., Samddar, P., & Kumar, P. (2018). "Green" synthesis of metals and their oxide nanoparticles: Applications for environmental remediation. *Journal of Nanobiotechnology*, *16*(1), 1–24. https://doi.org/10.1186/s12951-018-0408-4

Slman, D. K., Jalill, R. D. A., & Abd, A. N. (2018). Biosynthesis of zinc oxide nanoparticles by hot aqueous extract of allium sativum plants. *Journal of Pharmaceutical Sciences and Research*, *10*(6), 1590–1596.

Uikey, P., & Vishwakarma, K. (2016). Review of Zinc Oxide (Zno) Nanoparticles Applications and Properties. *International Journal of Emerging Technology in Computer Science & Electronics (IJETCSE)*, *21*(2), 976–1353.

Vasantharaj, S., Sathiyavimal, S., Saravanan, M., Senthilkumar, P., Gnanasekaran, K., Shanmugavel, M., Manikandan, E., & Pugazhendhi, A. (2019). Synthesis of ecofriendly copper oxide nanoparticles for fabrication over textile fabrics: Characterization of antibacterial activity and dye degradation potential. *Journal of Photochemistry and Photobiology B: Biology*, *191*(December 2018), 143–149. https://doi.org/10.1016/j.jphotobiol.2018.12.026

Wang, J., Deng, X., Zhang, F., Chen, D., & Ding, W. (2014). *ZnO nanoparticle-induced oxidative stress triggers apoptosis by activating JNK signaling pathway in cultured primary astrocytes*. 1–12.

Waris, A., Din, M., Ali, A., Afridi, S., Baset, A., Khan, A. U., & Ali, M. (2021). Green fabrication of Co and Co3O4nanoparticles and their biomedical applications: A review. *Open Life Sciences*, *16*(1), 14–30. https://doi.org/10.1515/biol-2021-0003

Wu, D., Wang, W., He, X., Jiang, M., Lai, C., Hu, X., Xi, J., & Wang, M. (2019). Biofabrication of nano copper oxide and its aptamer bioconjugate for delivery of mRNA 29b to lung cancer cells. *Materials Science and Engineering C*, *97*, 827–832. https://doi.org/10.1016/j.msec.2018.12.009

Zhang, L., Li, H., Yang, B., Zhou, Y., Zhang, Z., & Wang, Y. (2019). Photo-deposition of ZnO/Co3O4 core-shell nanorods with p-n junction for efficient oxygen evolution reaction. *Journal of Solid State Electrochemistry*, *23*(12), 3287–3297. https://doi.org/10.1007/s10008-019-04444-w